Food & Function

ROYAL SOCIETY OF CHEMISTRY

PAPER

View Article Online
View Journal | View Issue

Cite this: *Food Funct.*, 2025, **16**, 5008

Phyllanthus emblica L. polysaccharides mitigate obesity *via* modulation of lipid metabolism and gut microbiota in high-fat diet-fed mice†

Yi-Hsien Hsu,‡[a] Sheng-Yi Chen,‡[a] Jia-De Chen[a] and Gow-Chin Yen *[a,b]

Phyllanthus emblica L. polysaccharides (PEP) have been shown to ameliorate colitis through their antioxidant, anti-inflammatory, and gut microbiota-modulating properties. However, the potential of PEP in combating obesity remains unexplored. This study aimed to investigate the physicochemical characteristics of PEP and its mechanisms in modulating lipid metabolism in C57BL/6 mice treated with a high-fat diet (HFD). PEP is a high molecular weight, non-crystalline, sheet-like, heat-stable, α-acidic pyran polysaccharide rich in galactose and galacturonic acid. *In vivo* experiments demonstrated that administering PEP and atorvastatin (positive control) significantly reversed weight gain, adipose tissue hypertrophy, hyperlipidemia, liver steatosis, oxidative stress, and inflammation induced by a HFD. Mechanistically, PEP counteracted obesity by upregulating gene expression related to lipolysis (ATGL, HSL, and AMPKα), β-oxidation (SIRT1, PGC-1α, PPARα, CPT-1A, and MCAD), and cholesterol metabolism (LXRα and LXRβ), while downregulating the *de novo* lipogenesis axis (C/EBPα, PPARγ, SREBP1, ACC1, and FAS) and HMGCR, thereby enhancing fecal lipid excretion. Remarkably, PEP treatment decreased obesity-promoting bacteria (*Anaeroplasma* and *Clostridia_vadinBB60_group*) while increasing obesity-repressed flora (*Clostridium_sensu_stricto_1*, *Lactobacillus*, *Muribaculaceae*, *Romboutsia*, and *Turicibacter*). These changes correlated with increased production of short-chain fatty acids (SCFAs), which inhibited NF-κB *via* binding to GPR41/43. In summary, PEP promotes lipid metabolism and fecal fat excretion and exerts anti-inflammatory and antioxidant effects that are strongly linked to gut microbiota manipulation. These findings reveal the potential of PEP as a functional food ingredient for obesity prevention.

Received 26th March 2025,
Accepted 11th May 2025

DOI: 10.1039/d5fo01499a

rsc.li/food-function

1. Introduction

The Western pattern diet contributes to the development of obesity, which has become an epidemic globally. Approximately 890 million adults were obese worldwide in 2024.[1] An academic report suggests that without effective interventions, obesity rates could continue to rise, resulting in health and economic burdens projected to reach $3 trillion per year by 2030 and over $18 trillion by 2060.[1]

Diet plays a critical role in the development of obesity, leading to increased focus on the trillions of microbes residing in the human intestine and their potential impact on energy balance and metabolic signaling.[2,3] Polysaccharides are recognized for their ability to attenuate obesity, including the lowering of cholesterol levels, control of blood glucose, suppression of lipid accumulation, and exhibition of antioxidative and anti-inflammatory properties, as well as the reshaping of gut microbiota composition and the promotion of short-chain fatty acid (SCFA) production.[4] For instance, dietary supplementation of polysaccharides from *Anoectochilus Roxburghii* (Wall.) Lindl. significantly mitigated obesity through activation of the β-oxidation-related AMP-activated protein kinase (AMPK)/Sirtuin-1 (SIRT1)/Peroxisome proliferator-activated receptor gamma coactivator 1-alpha (PGC-1α) signaling pathway.[5] Also, polysaccharides directly improve lipid, cholesterol, and bile acid metabolism by promoting their excretion and upregulating lipolysis (ATGL, HSL, and AMPKα), β-oxidation (SIRT1, PGC-1α, PPARα, CPT-1A, and MCAD), and cholesterol metabolism (LXRα, LXRβ, and HMGCR)-related signaling while downregulating the *de novo* lipogenesis-related axis (C/EBPα, PPARγ, SREBP1, ACC1, and FAS).[4] Additionally, polysaccharides are not readily digested in the small intestine but are fermented by the colonic microbiota to produce the end products of SCFAs.[6] SCFAs have garnered significant attention due to

[a]*Department of Food Science and Biotechnology, National Chung Hsing University, 145 Xingda Road, Taichung 40227, Taiwan. E-mail: gcyen@nchu.edu.tw*
[b]*Advanced Plant and Food Crop Biotechnology Center, National Chung Hsing University, Taichung 40227, Taiwan*

†Electronic supplementary information (ESI) available. See DOI: https://doi.org/10.1039/d5fo01499a

‡These authors contributed equally to this work.

their ability to inhibit oxidative stress, inflammatory cascades, and lipid accumulation through engagement with their receptors GPR41/GPR43, which mediate NF-κB and AMPK signaling, respectively.[7] Accordingly, bioactive polysaccharides are promising options for preventing or treating obesity.

Phyllanthus emblica Linn., commonly known as amla or Indian gooseberry, is widely distributed in India, Malaysia, the Philippines, China, and Thailand. It contains abundant functional components, including phenolic acids, flavonoids, sterols, tannins, triterpenoids, amino acids, vitamins, and polysaccharides.[8] Previous reports have shown that *Phyllanthus emblica* L. fruit extract and its major bioactive compound, gallic acid, effectively mitigate obesity by restraining methylglyoxal-associated leptin resistance, oxidative stress, inflammation, and dysbiosis in high-fat diet (HFD)-fed rats.[9–11] As well, *Phyllanthus emblica* L. polysaccharides (PEP) enhance the abundance of SCFA-producing bacteria (*Romboutsia*, *Clostridium_sensu_stricto_1*, and *Lactobacillus*) and consequently exhibit antioxidant and anti-inflammatory activities by increasing the levels of SCFAs, anti-inflammatory cytokines (IL-4 and IL-10), and antioxidant enzymes (SOD, catalase, and GPx) while downregulating the activation of the RAGE/NF-κB pathway in colitis rats subjected to TNBS treatment.[11]

Several key mediators are involved in lipid metabolism, including those regulating lipolysis, β-oxidation, cholesterol metabolism, and the *de novo* lipogenesis pathway. To date, no study has comprehensively explored the effects of PEP on lipid metabolism *via* underlying mechanisms. Therefore, this study aimed to clarify how PEP protects against HFD-induced obesity through mechanisms involving lipid metabolism and gut microbiota modulation. The results are expected to provide a basis for developing PEP as a dietary supplement to improve obesity.

2. Materials and methods

2.1. Chemicals

Propionic acid, 1-phenyl-3-methyl-5-pyrazolone (PMP), trichloroacetic acid, rhamnose, galactose, mannose, galacturonic acid, arabinose, fucose, glucose, glucuronic acid, and atorvastatin (ATR) were purchased from Sigma-Aldrich (St. Louis, MO, USA). Butyric acid was purchased from Alfa Aesar (Haverhill, MA, USA). Acetic acid and 95% ethanol were purchased from Echo Chemical (Miaoli, Taiwan). The RNA extraction reagent was purchased from EBL Biotechnology (Taipei, Taiwan). Refined beef tallow was purchased from President Nisshin Corp. (Tainan, Taiwan). cDNA primers were purchased from Genomics Biotechnology Co. (Taipei, Taiwan).

2.2. Preparation of PEP

Phyllanthus emblica L. fruits were obtained from Yungtai Orchard Co., Ltd (Taichung, Taiwan). The preparation of PEP was based on methods from a previous study.[11] Briefly, the fruit powders were homogenized with ddH_2O at a solid–liquid ratio of 1 : 20 (g mL^{-1}). The mixture underwent extraction through heating and stirring at 90 °C for 120 min using a rotating stirrer (RW20 DZM, IKA Werke GmbH & Co., Staufen im Breisgau, Germany). The polysaccharide-rich supernatant was collected. Subsequently, four volumes of 95% ethanol were added to the supernatant to induce precipitation at 4 °C for 24 h. After centrifugation, the precipitate was resolubilized and subjected to dialysis (with a cutoff of 6–8 kDa) for 48 h. Finally, the material was lyophilized to obtain PEP.

2.3. Physical and structural characteristics of PEP

Following established procedures outlined in a previous study,[11] the analysis of the physical and structural characteristics of PEP was entrusted to the Department of Chemical and Materials Engineering at the National Yunlin University of Science and Technology (Yunlin, Taiwan).

2.4. Molecular weight analysis

Following the established procedures outlined in a previous study,[11] the molecular weight of PEP was analyzed using high-performance liquid chromatography coupled with gel permeation chromatography (HPLC-GPC), employing SB-805 HQ plus SB-804 HQ columns (Shodex OHpak, New York, NY, USA). PEP was dissolved in ddH_2O at a 6 mg mL^{-1} concentration and analyzed with an RI-1530 detector (JASCO, Tokyo, Japan). A standard curve was constructed using pullulan to determine the molecular weight of PEP.

2.5. Monosaccharide composition determination

The monosaccharide compositions of PEP were analyzed using the method outlined in a prior study.[11] Briefly, PEP was derivatized with a 0.5 M PMP solution at 70 °C for 2 h. The PMP derivatives were diluted with ddH_2O and filtered through a 0.22 μm membrane. The same derivatization procedure was applied to monosaccharide standards, including mannose, rhamnose, glucuronic acid, galacturonic acid, glucose, galactose, arabinose, and fucose. PMP derivatives were analyzed using a Hitachi Chromaster HPLC system equipped with a 5110 pump, a 5210 autosampler, a 5310 column oven, and a 5430 diode array detector (Hitachi, Tokyo, Japan). A LiChrospher® 100 RP-18 column (250 mm × 4 mm, 5 μm) (Merck, Darmstadt, Hessen, Germany) was used for separation. The mobile phase consisted of liquid A (0.1 M phosphate buffer solution, pH 7.5) and liquid B (acetonitrile). The solvent gradient elution program began at 88% A/12% B and transitioned to 86% A/14% B over 0 to 35 minutes. It then shifted from 86% A/14% B to 84% A/16% B between 35 and 36 min, maintaining this ratio from 36 to 54 min. The gradient was subsequently adjusted back to 88% A/12% B from 54 to 56 min, with this final composition held constant until 58 min. The elution was carried out at a flow rate of 1.1 mL min^{-1}, with an injection volume of 20 μL, and detection was performed at a UV wavelength of 250 nm.

2.6. Animal experiments

Male C57BL/6 mice (7 weeks old and weighing 22 ± 1.5 g) were obtained from the BioLASCO Experimental Animal Center

(Taipei, Taiwan). The mice were housed under controlled conditions: a temperature of 24 ± 2 °C, relative humidity of 55 ± 5%, and a 12 h light–dark cycle. They were provided free access to the Lab5001 diet (Purina Mills, St. Louis, MO, USA) and RO water.

Following a one-week acclimation, the mice were randomly divided into six groups (n = 5 per group): control group (Lab5001 diet), HFD group (40% beef tallow), ATR group (HFD + atorvastatin 20 mg per kg b.w., positive control), L-PEP group (HFD + low dose of PEP 50 mg per kg b.w.), M-PEP group (HFD + medium dose of PEP 100 mg per kg b.w.), and H-PEP group (HFD + high dose of PEP 200 mg per kg b.w.), with dosages based on a previous report.[12]

PEP or ATR was administered daily at 2 p.m. *via* intragastric administration for 8 weeks. Mice in the control and HFD groups received an equivalent volume of RO water. Throughout the study, body weight and food intake were monitored. In the final week, feces were collected. Mice were sacrificed by anesthetizing them with 3% isoflurane until respiration ceased in a closed container. Samples (blood samples, liver tissue, and white adipose tissue) were collected following euthanasia of the mice for subsequent analyses. This study was conducted following the guidelines approved by the Institutional Animal Care and Use Committee (IACUC) of National Chung Hsing University under application number 111-116.

2.7. Serum biochemical analysis

Biochemical marker analysis was entrusted to the National Laboratory Animal Center (NLAC) (NARLabs, Taiwan). In short, the levels of total cholesterol (TC), total triglyceride (TG), low-density lipoprotein cholesterol (LDL-C), alanine aminotransferase (ALT), and aspartate aminotransferase (AST) in serum were measured using a Hitachi 7180 biochemical analyzer (Tokyo, Japan).

2.8. Oral glucose tolerance test (OGTT)

In the 8th week, an oral glucose tolerance test (OGTT) was conducted. Blood samples were collected from the tail vein of mice after an 8 h fast. Initially, fasting blood glucose levels were measured. Subsequently, a glucose solution (2 g per kg body weight) was administered intragastrically to the mice. After glucose administration, blood glucose levels were monitored at 15, 30, 60, 90, and 120 min using the OneTouch® Ultra Plus Flex glucometer (LifeScan, Inc., Milpitas, CA, USA). The area under the curve (AUC) for blood glucose levels was calculated to assess glucose tolerance. The AUC between any two time points was determined using the formula: AUC = Δtime × [(glucose level$_{time1}$ + glucose level$_{time2}$)/2].

2.9. Histological examinations

Hematoxylin and eosin (H&E) staining of liver tissues and epididymal adipose tissues was performed by the Animal Disease Diagnostic Center (ADDC), College of Veterinary Medicine, National Chung Hsing University (Taichung, Taiwan), and verified by Prof. Jiunn-Wang Liao. The epididymal adipose and liver tissues were fixed in 10% formalin at the time of sacrifice. After fixation, the samples were embedded in paraffin at −20 °C and sectioned. Finally, the tissue sections were stained with H&E for microscopic examination and analysis.

2.10. Antioxidant and cytokine analysis

Liver tissues were homogenized with lysis buffer using an SH-100 tissue homogenizer (Kurabo, Osaka, Japan). According to the manufacturer's instructions, protein concentrations were determined using the Bicinchoninic Acid (BCA) assay (BC03-500, Visual Protein, Taipei, Taiwan). For antioxidant measurements, ELISA kits for catalase (CAT, 707002), superoxide dismutase (SOD, 706002), and glutathione peroxidase (GPx, 703102) were obtained from Cayman Chemicals (Ann Arbor, MI, USA). Cytokine levels in liver tissue, including IL-1β (DY401), IL-10 (DY417), IL-6 (DY406), IL-4 (DY404), and TNF-α (DY410), were analyzed using ELISA kits from R&D Systems (Minneapolis, MN, USA). All tests followed the respective manufacturer's guidelines for the above analyses.

2.11. Malondialdehyde (MDA) content analysis

A sample of 150 μL of liver tissue homogenate was mixed with 300 μL of the TCA-TBA-HCl reagent (15% trichloroacetic acid in 0.25 N HCl and 0.375% 2-thiobarbituric acid in 0.25 N HCl). The mixture was heated in a dry bath at 100 °C for 15 min and then cooled, and 300 μL of butanol was added. After centrifuging at 2000 rpm for 10 min, 100 μL of the pink supernatant was collected, and its absorbance was measured at 535 nm. 1,1,3,3-Tetraethoxypropane was used as the standard to construct a calibration curve and calculate the concentration of MDA content.[11]

2.12. Analysis of fecal lipid excretion

The analysis of fecal lipid excretion was conducted according to the method described in a previous report.[11] Briefly, fecal lipids were extracted from dried fecal powder using a chloroform solution (2 : 1, v : v). Total lipids were measured gravimetrically. Fecal triglycerides (TGs), cholesterol, and total bile acids (TBAs) were measured using the fecal TG assay kit (E-BC-K261-M, Elabscience, Wuhan, China), total bile acids assay kit (E-BC-K181-M, Elabscience, Wuhan, China), and cholesterol CHOD PAP assay kit (BXC0261A, Fortress Diagnostics, Antrim, Ulster, UK) respectively, following the manufacturers' guidelines.

2.13. Quantitative real-time polymerase chain reaction (real-time qRT-PCR)

qRT-PCR was conducted using the methods previously described.[11] In brief, total RNA was extracted from liver and epididymal adipose tissues using the TRIzol reagent. RNA concentration was quantified using a NanoDrop 1000 spectrophotometer (Thermo Scientific, Waltham, USA). cDNA was synthesized using a ZEJUScript II RT kit (ZEJU Bio-Technology, Kaohsiung, Taiwan). qRT-PCR was performed using a StepOne™ PCR system (Applied Biosystems, Foster City, CA) with 2× Universal SYBR Green Fast qPCR Mix (RM21203,

ABclonal, Woburn, MA, USA). The qRT-PCR conditions were as follows: initial denaturation at 95 °C for 15 min, followed by denaturation at 95 °C for 10 s, annealing at 54–64 °C for 20–30 s, and extension at 72 °C for 45 s. Relative gene expression levels were calculated using the $2^{-\Delta\Delta CT}$ method, with normalization to the expression of the internal reference (housekeeping) gene. The primer sequences and annealing temperatures used are provided in Table S1.†

2.14. Short-chain fatty acid (SCFA) analysis by HPLC

SCFA analysis followed previously established protocols, including acetic acid, propionic acid, and butyric acid.[13] In brief, fecal samples from mice were mixed with ethanol and centrifuged. The supernatant was combined with derivatization reagents (pyridine, 1-EDC hydrochloride, and 2-NPH-HCl) to form fatty acid hydrazides. The derived compounds were analyzed using the Hitachi Chromaster HPLC system (Hitachi, Tokyo, Japan) equipped with a LiChrospher® 100 RP-18 column (250 mm × 4 mm, 5 μm) (Merck, Darmstadt, Hessen, Germany). The elution system consisted of liquid A (ddH_2O containing 0.1% TFA, adjusted to pH 4.5) and liquid B (acetonitrile/methanol, 2 : 1, with 0.1% TFA adjusted to pH 4.5). Flowing at a rate of 1.0 mL per min, 20 μL injection volumes were used, and a detector was performed at 400 nm. SCFA concentrations were quantified relative to 2-ethylbutyric acid reference standards.

2.15. Gut microbiota analysis

DNA extraction, gut microbiota analysis, and Spearman's correlation analysis were entrusted to AllBio Science, Inc. (Taichung, Taiwan). Following the established methods described in a previous study,[13] genomic DNA was extracted from fecal samples using the AllPure Genomic DNA Extraction Kit. DNA quantification was performed with a Qubit 2.0 Fluorometer (Invitrogen, Carlsbad, CA, USA). Next-generation sequencing (NGS) targeted the V3–V4 hypervariable regions of 16S rDNA for taxonomic analysis. The V3 and V4 regions were amplified using the forward primer "CCTAGGRRBGCASCAGKVRVGAAT" and the reverse primer "GGACTACNVGGGTWTCTAATCC". DNA library construction and sequencing (Silva_138) were employed to ensure sequence quality control and merge reads, grouping sequences with over 97% similarity. Allbio conducted all analyses and performed network visualization using Cytoscape 3.10.2 (Boston, MA, USA).

2.16. Statistical analysis

PEP composition analyses were presented as means ± standard deviation (SD), and animal study analyses were presented as means ± standard error of the mean (SEM). All the statistical analyses were performed using one-way analysis of variance (ANOVA), followed by *post hoc* analysis with Duncan's multiple comparison tests using the Statistical Package for the Social Sciences (SPSS) version 20 software (IBM Corporation, Armonk, New York, USA). The p-value < 0.05 was considered statistically significant.

3. Results

3.1. Physicochemical characteristics of PEP

As shown in Fig. 1A and B, GPC analysis revealed the major peaks of PEP corresponding to molecular weights of 1518.43 kDa (96.5%) and 14.05 kDa (3.5%). The monosaccharide composition analysis showed that PEP was composed of mannose, rhamnose, glucuronic acid, galacturonic acid, glucose, galactose, and arabinose (molar ratio: 1.19 : 1.00 : 1.27 : 2.30 : 2.00 : 8.31 : 3.63) (Fig. 1C and D). FTIR analysis of PEP revealed functional groups of O–H (around 3440 cm^{-1}), C–H (around 2923 cm^{-1}), ester groups (–COOR around 1745 cm^{-1}), carboxylate ions (–COO around 1634 cm^{-1}), C–H (around 1385 cm^{-1}), C–O–C and C–O–H (the "fingerprint region" of polysaccharides around 1022–1103 cm^{-1}), and the β-linked glycosyl residues (around 916 cm^{-1}) (Fig. 2A), indicating that PEP contains uronic acid residues and pyranose rings.[14,15] XRD and SEM analyses indicated that PEP has a non-crystalline, sheet-like, and tightly packed cross-sectional microstructure (Fig. 2B and D). Additionally, thermal analysis using DSC showed a peak temperature of 102.7 °C. At the same time, TGA results showed that PEP can withstand temperatures up to 260 °C, with two major weight loss events occurring at 20–120 °C and around 260 °C, indicating that PEP exhibits heat-stable properties suitable for application in the food industry (Fig. 2E and F). The glycosidic linkages of PEP will be investigated in future studies using gas chromatography-mass spectrometry (GC-MS) and nuclear magnetic resonance (NMR) spectroscopy.

3.2. PEP attenuated HFD-induced obesity symptoms and fat accumulation

In Fig. 3A, the design of the animal experiment and treatment is illustrated. The photographs show that the body shape of mice was more prominent in the HFD group than in the other groups (Fig. 3B). The highest body weight and weight gain were consistently found under HFD conditions, while PEP and atorvastatin administration significantly reduced those in mice subjected to HFD treatment (Fig. 3C and D). Additionally, the PEP and atorvastatin consumption decreased food and energy intake in HFD-treated mice (Fig. 3E and F). As anticipated, fat hyperplasia (epididymal, mesenteric, and perinephric adipose tissues) was dramatically increased within HFD-treated mice, whereas it was repressed by PEP and atorvastatin treatment (Fig. 4A). Furthermore, the quantification results showed that the weight and percentage of adipose tissue were significantly increased in mice fed a HFD alone, which was effectively inhibited by PEP and atorvastatin treatment, particularly in epididymal adipose tissue (Table 1). In addition, immune cell infiltration in the hypertrophic H&E-stained epididymal adipose tissue was observed in HFD-induced mice; this phenomenon was ameliorated by PEP and atorvastatin intake (Fig. 4B). The size and diameter of epididymal adipose tissues were significantly enlarged in HFD-fed mice compared with the control group (Fig. 4C and D). Administration of PEP and atorvastatin suppressed the hypertrophy of epididymal adipose tissues in mice subjected to HFD treatment (Fig. 4C and D).

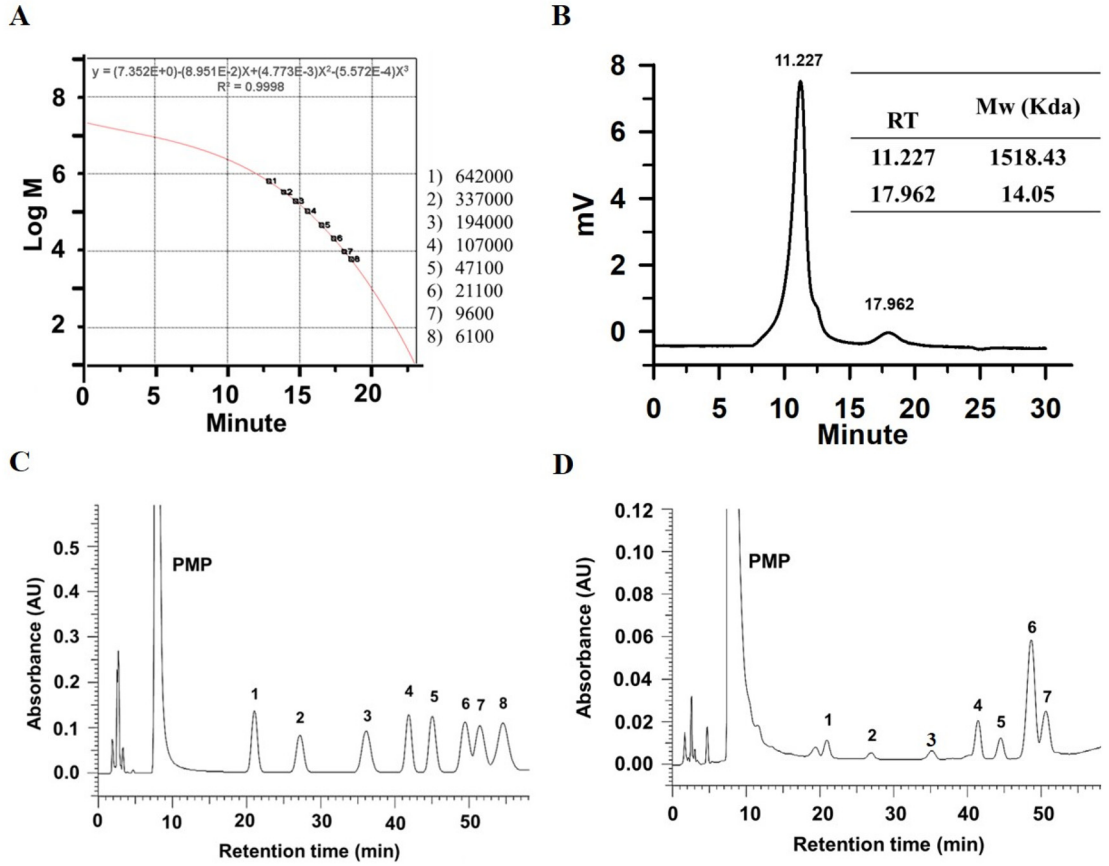

Fig. 1 Molecular weight and monosaccharide composition of PEP. (A) Standard curve of pullulan. (B) The molecular weight of PEP. (C) Monosaccharide standards. (D) Monosaccharide composition of PEP. The peaks correspond to the following monosaccharide standards: 1. mannose, 2. rhamnose, 3. glucuronic acid, 4. galacturonic acid, 5. glucose, 6. galactose, 7. arabinose, and 8. fucose.

3.3. PEP administration attenuated HFD-induced liver injury, glucose intolerance, and lipid storage

As shown in Fig. 5A, fat deposition in the liver was observed under HFD conditions but was reversed after PEP and atorvastatin treatment. Additionally, PEP and atorvastatin protected against HFD-induced liver injury by reducing ALT and AST levels (Fig. 5B and C), indicating that PEP did not induce hepatotoxicity. HFD-induced obesity often accompanies glucose intolerance. To examine the regulatory effects of PEP on glucose tolerance, we performed an OGTT in the animal experiment. After administering 2 g kg^{-1} of glucose, the HFD and ATR groups exhibited higher blood glucose levels at 15 min. However, the HFD group showed a smaller decrease in blood glucose levels at 30 min, indicating impaired glucose tolerance compared to the control group. In contrast, the ATR and PEP groups had lower blood glucose levels than the HFD group after 15 min (Fig. 5D). Additionally, the AUC analysis revealed that the HFD group had a significantly higher AUC than the control group, which was significantly decreased in the ATR and PEP groups (Fig. 5E). In addition, HFD significantly increased serum TG, TC, and LDL-C levels relative to the control group, which were effectively decreased by atorvastatin and PEP administration (Fig. 6A–C). The serum lipid-lowering effect of polysaccharides is associated with their ability to promote fat excretion in feces.[4] As shown in Fig. 6D–G, mice fed with 200 mg per kg b.w. of PEP significantly increased fecal fat, TG, TC, and TBA contents compared to the HFD group.

3.4. PEP administration alleviated hepatic oxidative stress and inflammatory reaction

It has been documented that HFD promotes inflammation and oxidative stress in obese mice.[10] Here, HFD induced oxidative stress by enhancing hepatic MDA levels and reducing catalase, SOD, and GPx activities when measured against the untreated mice (Fig. 7A–D). PEP and atorvastatin administration significantly decreased MDA levels and increased catalase, SOD, and GPx activities compared to the HFD group (Fig. 7A–D). Additionally, the HFD group exhibited high expression of the inflammatory mediator NF-κB p65 gene combined with lower IκBα expression (Fig. 8A and B), indicating that a hepatic inflammatory response was triggered in mice subjected to HFD treatment. Conversely, the PEP and atorvastatin administration reversed this tendency in NF-κB p65 and IκBα levels (Fig. 8A and B). These phenomena were validated by examining the protein expression of pro-inflammatory and

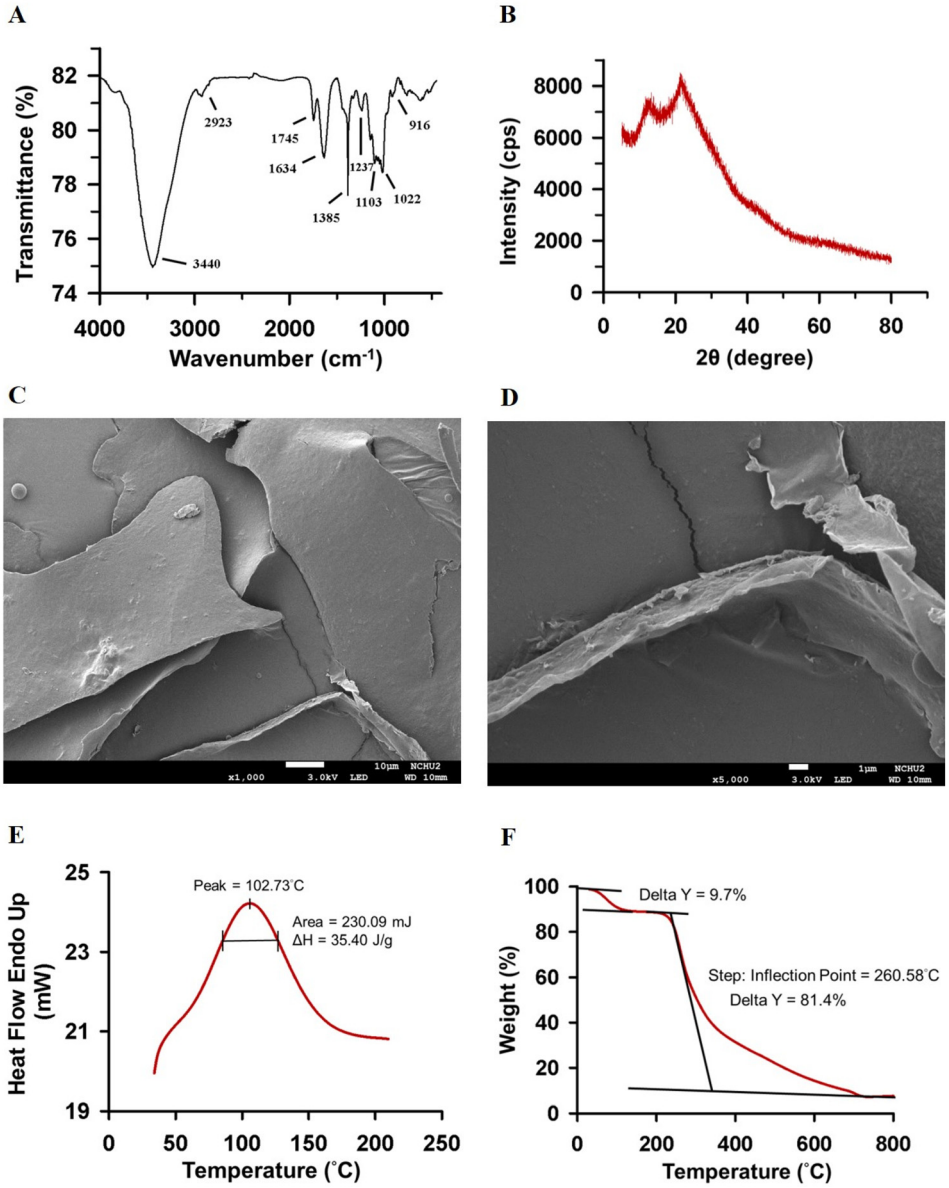

Fig. 2 Physicochemical characteristics of PEP. (A) Functional groups of PEP were determined by FTIR spectrometry. (B) Crystal properties evaluated by XRD. Microstructure of PEP at (C) 1000× and (D) 5000× magnification was captured using FE-SEM. Thermodynamic characteristics of PEP were determined by (E) DSC and (F) TGA.

anti-inflammatory cytokines. The HFD group had significantly lower levels of anti-inflammatory cytokines (IL-4 and IL-10) and higher levels of pro-inflammatory cytokines (TNFα, IL-1β, and IL-6) compared to the control group (Fig. 8C–G). The ATR and PEP groups showed suppressed levels of pro-inflammatory cytokines and elevated levels of anti-inflammatory cytokines compared to the HFD group (Fig. 8C–G).

3.5. PEP regulated lipolysis, β-oxidation, cholesterol metabolism, and *de novo* lipogenesis-related axis

AMPK is crucial for maintaining energy balance and regulating lipid metabolism.[16] As shown in Fig. 9A–C, the gene expression of lipolysis-related pathways (ATGL, HSL, and AMPKα) was significantly decreased in the HFD group as opposed to the control group. Administering atorvastatin and PEP effectively enhanced lipolytic capacity by upregulating ATGL, HSL, and AMPKα gene expression in HFD-fed mice (Fig. 9A–C). Noteworthily, the HFD-induced reduction in mRNA expression of β-oxidation genes (SIRT1, PGC-1α, PPARα, CPT-1A, and MCAD) was rescued by atorvastatin and PEP treatment, specifically in the H-PEP group (Fig. 9D–H). Consistently, the HFD-evoked activation of the *de novo* lipogenesis-related axis (C/EBPα, PPARγ, SREBP1, ACC1, and FAS) was significantly inhibited by atorvastatin and PEP supplementation (Fig. 10A–E). Bile acid and cholesterol excretion are closely linked to maintaining cholesterol homeostasis

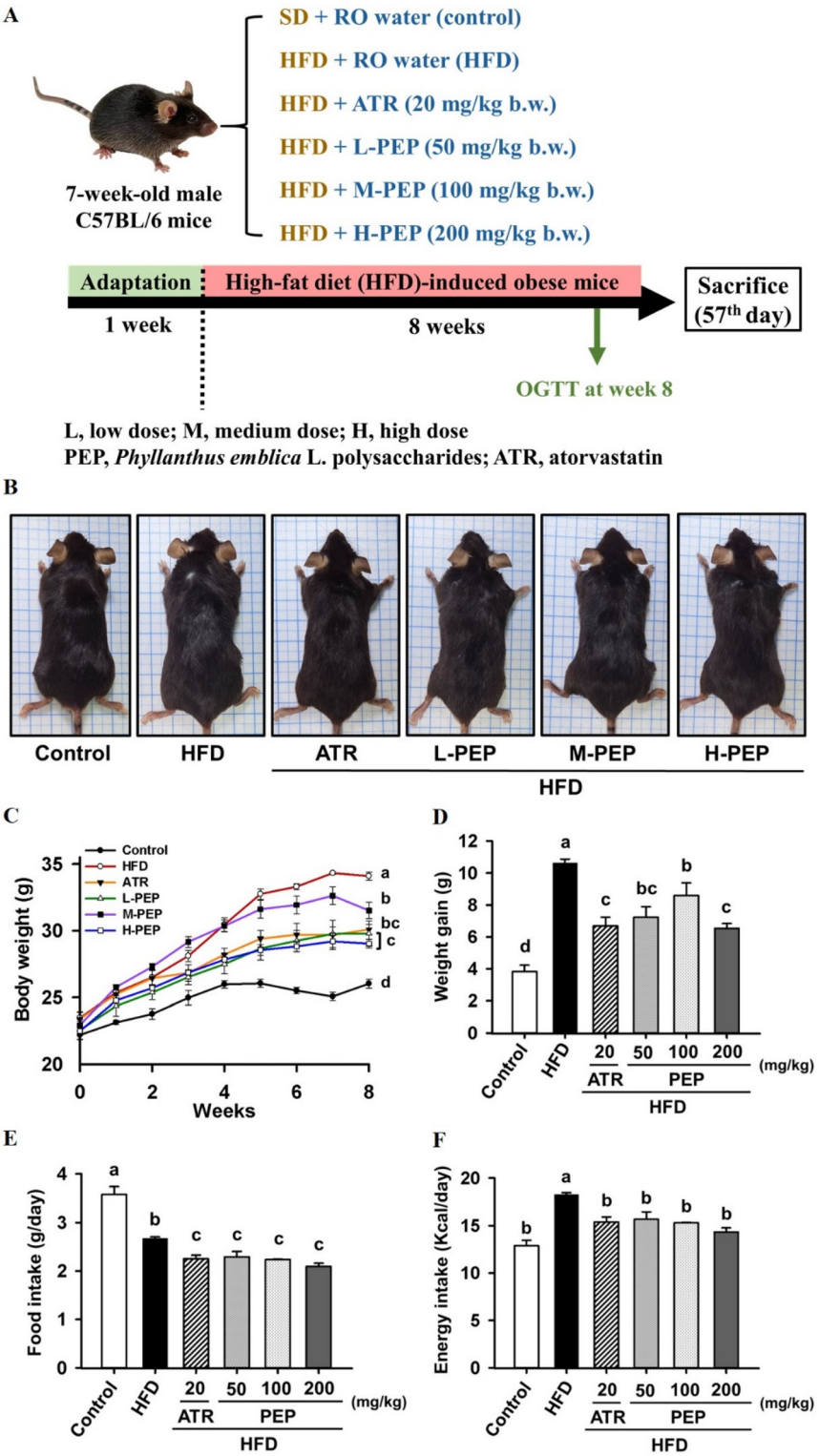

Fig. 3 Effect of PEP administration on body shape and animal weight in HFD-induced obese mice. (A) An illustration of experimental grouping. (B) Body shape of mice. (C) Body weight. (D) Weight gain. (E) Food intake. (E) Energy consumption. Columns with different lowercases are significantly different ($p < 0.05$).

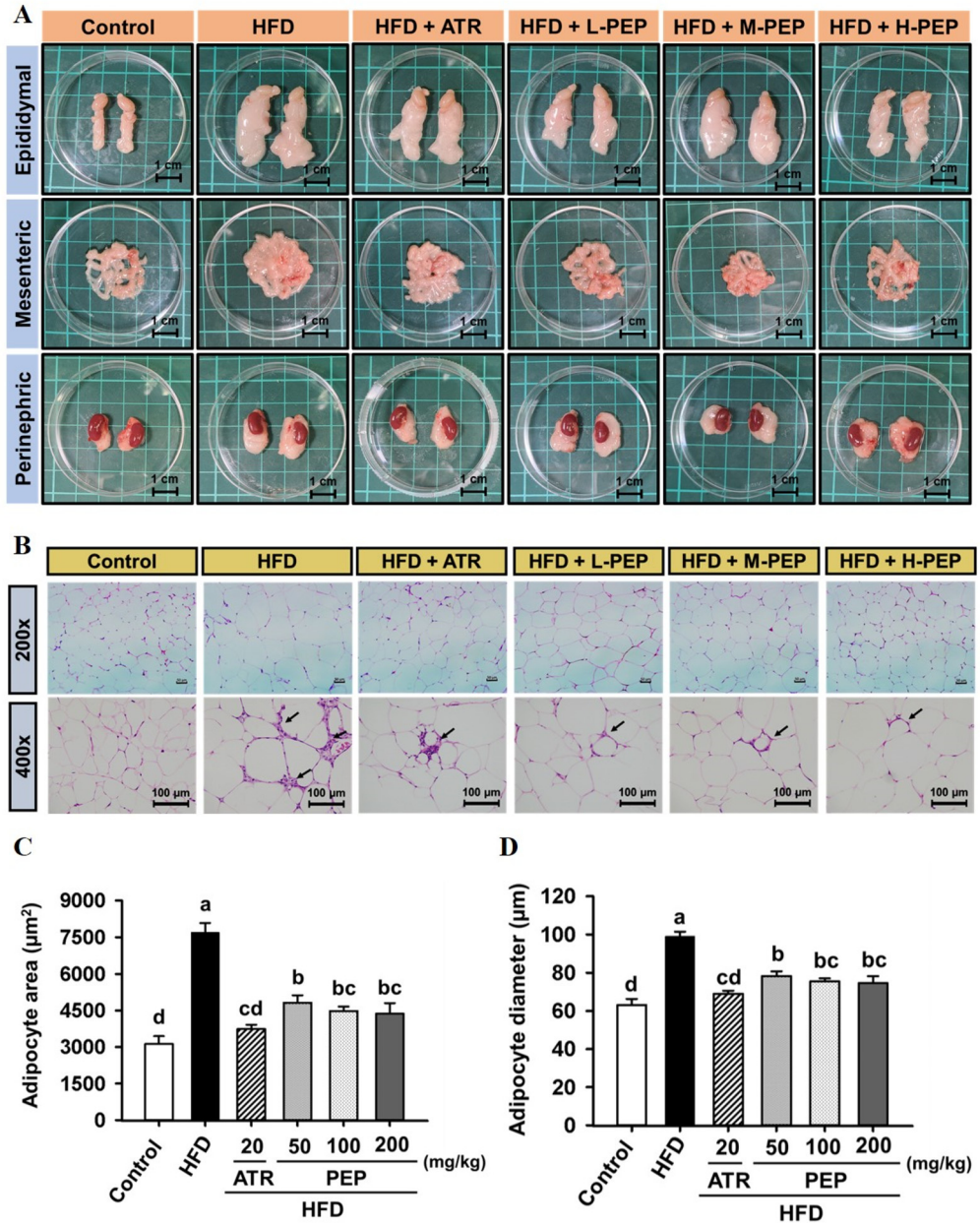

Fig. 4 Effect of PEP administration on fat hypertrophy and hyperplasia in HFD-induced obese mice. (A) Photographs of representative adipose tissues from each group. (B) Immune cell infiltration in epididymal adipose tissue (indicated by arrows). (C) Size of epididymal adipocytes in epididymal adipose tissue. (D) Diameter of epididymal adipocytes in epididymal adipose tissue. Columns with different lowercase letters are significantly different ($p < 0.05$).

Table 1 Effect of PEP administration on the weight of adipose tissues in HFD-induced obese mice[a]

	Control	HFD	HFD + ATR	HFD + L-PEP	HFD + M-PEP	HFD + H-PEP
BW (g)	26.02 ± 0.35^{d}	34.09 ± 0.30^{a}	30.08 ± 0.37^{bc}	29.79 ± 0.95^{c}	31.51 ± 0.62^{b}	29.03 ± 0.32^{c}
EFW (g)	0.32 ± 0.02^{d}	1.73 ± 0.08^{a}	0.94 ± 0.03^{c}	1.07 ± 0.14^{c}	1.39 ± 0.08^{b}	1.16 ± 0.10^{bc}
MFW (g)	0.36 ± 0.01^{b}	0.63 ± 0.02^{a}	0.54 ± 0.02^{a}	0.52 ± 0.07^{a}	0.53 ± 0.06^{a}	0.055 ± 0.01^{a}
PFW (g)	0.13 ± 0.02^{d}	0.48 ± 0.04^{ab}	0.35 ± 0.03^{c}	0.40 ± 0.04^{bc}	0.53 ± 0.04^{a}	0.41 ± 0.03^{bc}
Total body fat (g)	0.82 ± 0.02^{d}	2.80 ± 0.12^{a}	1.83 ± 0.05^{c}	1.98 ± 0.24^{c}	2.47 ± 0.15^{ab}	2.13 ± 0.11^{bc}
EFW/BW (%)	1.24 ± 0.08^{d}	5.29 ± 0.30^{a}	3.37 ± 0.09^{c}	3.66 ± 0.55^{bc}	4.37 ± 0.26^{b}	4.04 ± 0.24^{bc}
MFW/BW (%)	1.37 ± 0.07^{c}	1.93 ± 0.07^{a}	1.77 ± 0.05^{ab}	1.60 ± 0.15^{bc}	1.67 ± 0.15^{ab}	1.96 ± 0.07^{a}
PFW/BW (%)	0.41 ± 0.05^{c}	1.42 ± 0.12^{a}	1.17 ± 0.11^{b}	1.30 ± 0.12^{b}	1.67 ± 0.10^{ab}	1.47 ± 0.11^{ab}
Body fat ratio	3.10 ± 0.05^{c}	8.50 ± 0.42^{a}	6.88 ± 0.31^{b}	6.61 ± 0.76^{b}	7.77 ± 0.36^{ab}	7.51 ± 0.30^{ab}

[a] Value with different lowercases indicate a statistically significant difference at $p < 0.05$ ($n = 5$). BW, body weight; EFW, epididymal fat weight; MFW, mesenteric fat weight; PFW, perinephric fat weight.

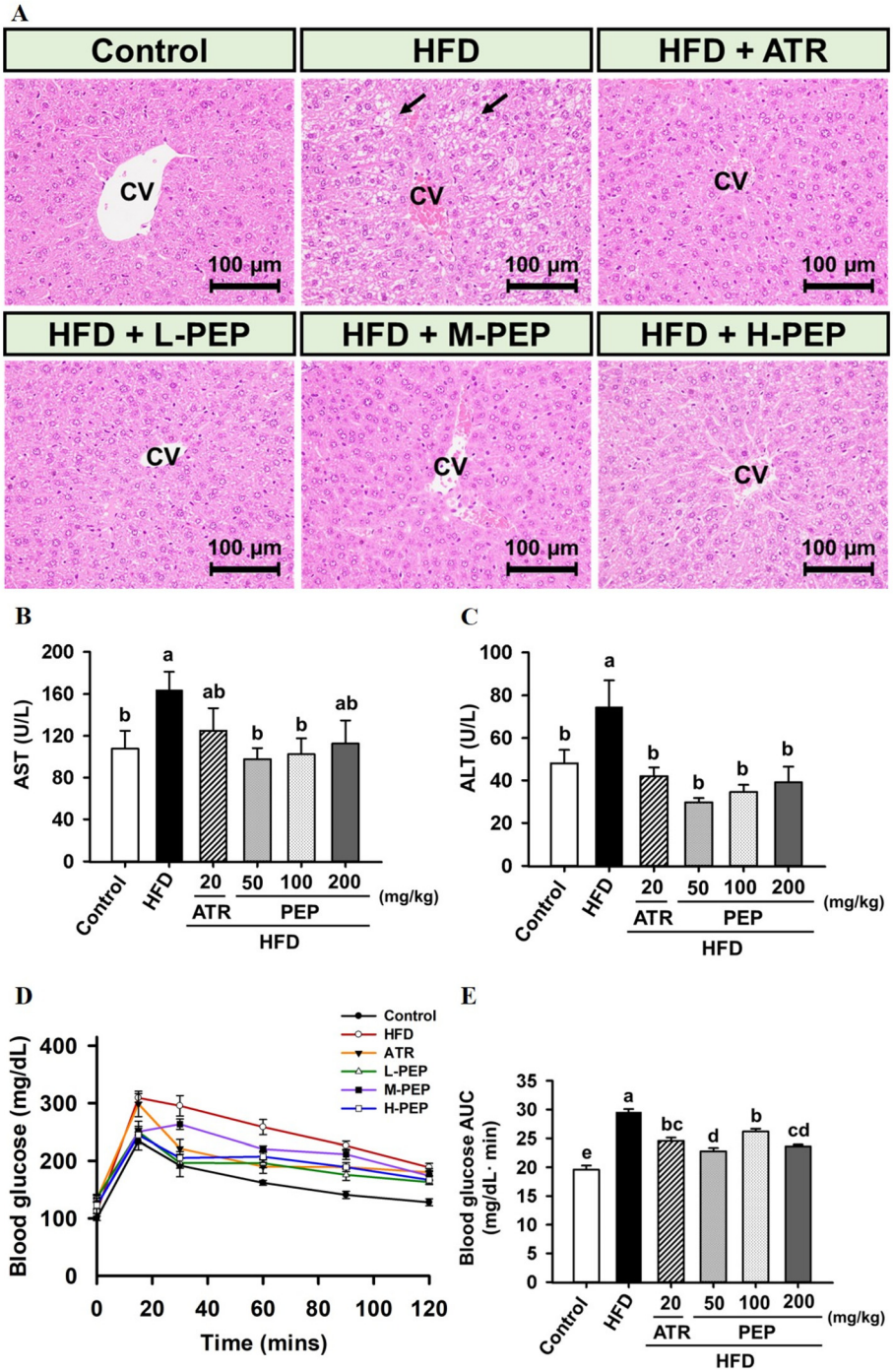

Fig. 5 Effect of PEP administration on liver function and glucose tolerance in HFD-induced obese mice. (A) Liver histology at 400× magnification, with arrows indicating fat accumulation with micro-vesicles. CV represents the central vein. (B) AST levels. (C) ALT levels. (D) Time curves of the OGTT. (E) AUC values for each group of mice. Columns with different lowercase letters are significantly different ($p < 0.05$).

and metabolism.[17] In agreement with the results of fecal lipids and bile acid excretion, intake of atorvastatin and PEP upregulated cholesterol metabolism-related genes (LXRα and LXRβ) and downregulated the cholesterol synthesis-mediated gene (HMGCR) in mice subjected to HFD treatment (Fig. 10F–H), suggesting that PEP effectively regulates lipid metabolism.

3.6. PEP modulated gut microbiota composition and promoted SCFA production

Polysaccharides combat obesity by altering intestinal microbiota composition and enhancing SCFA production, which directly or indirectly modulates AMPK-related lipid metabolism pathways, oxidative stress, and inflammatory response

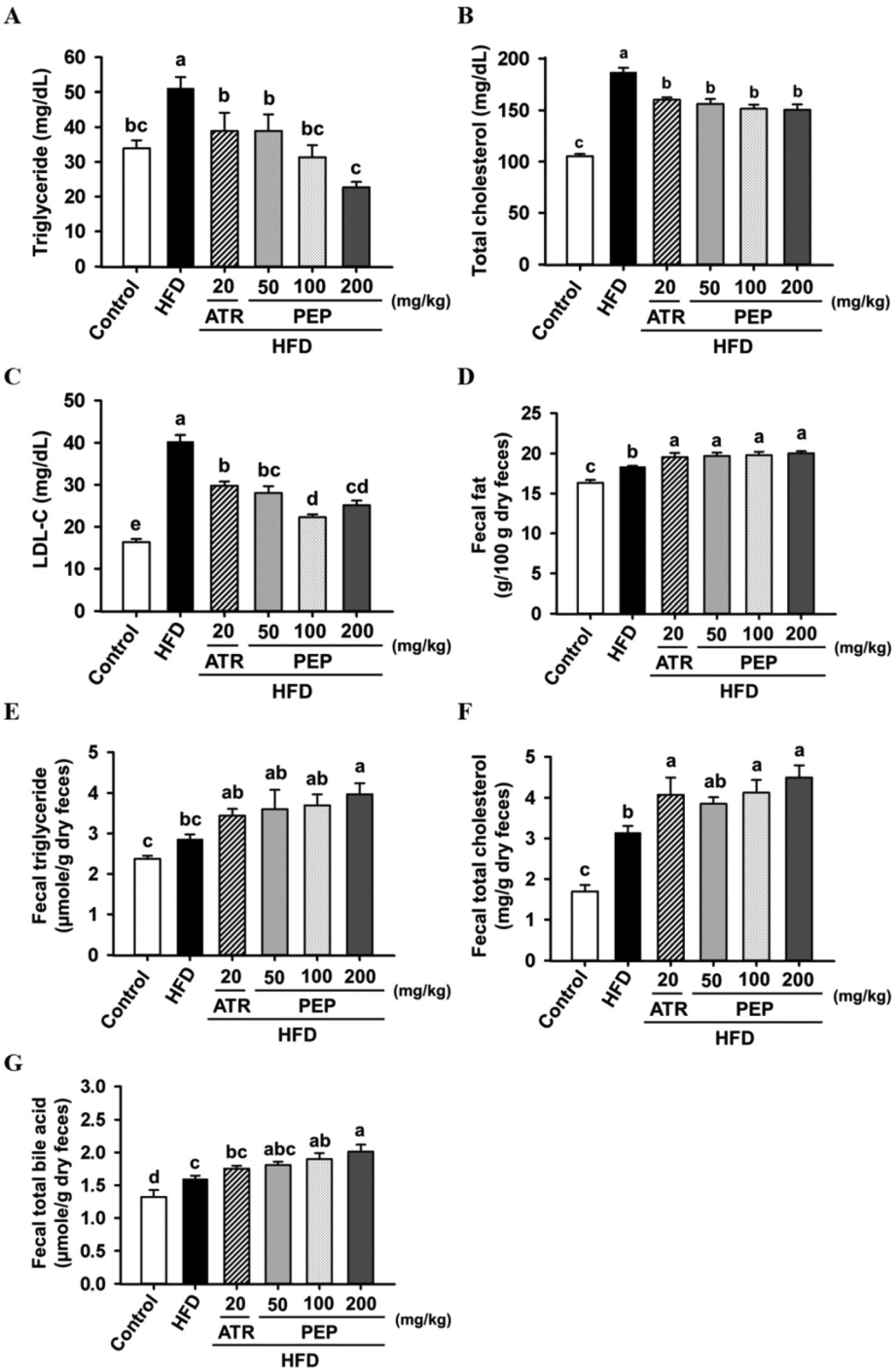

Fig. 6 Effect of PEP administration on serum lipid levels and fecal lipid excretion in HFD-induced obese mice. (A–C) The levels of serum TG, TC, and LDL-C. (D–G) The excretion levels of fecal lipids, TG, TC, and TBA. Columns with different lowercase letters are significantly different ($p < 0.05$).

via engagement with GPR41/GPR43 receptors.[4] As shown in Fig. 11A, *Anaerotruncus* dominated the HFD group at the genus level, an opportunistic pathogen strongly linked to obesity markers, including serum lipids and inflammation,[18] suggesting that HFD evoked dysbiosis; in contrast, H-PEP administration was dominated by *g_Romboutsia*, which is positively correlated with SCFA production.[11] At the genus level, *Turicibacter*, *Clostridium_sensu_stricto_1*, and *Romboutsia* had higher relative abundance in the PEP groups than in the HFD group, likely contributing to the anti-obesity effect (Fig. 11B–E). Conversely, PEP and atorvastatin reduced the relative abundance of *Mucispirillum*, *Erysipelatoclostridium*, and *Candidatus_Arthromitus* in mice (Fig. 11F–H).

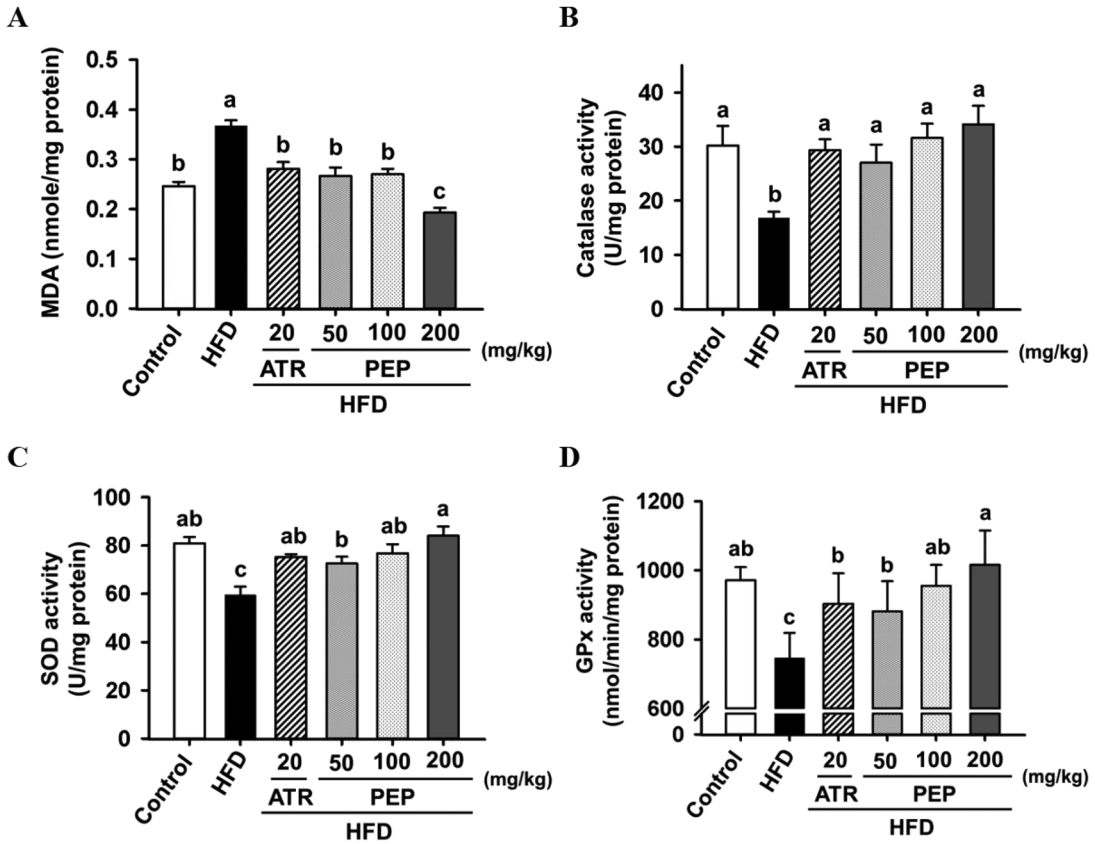

Fig. 7 Effect of PEP administration on hepatic antioxidant enzymes in HFD-induced obese mice. (A) MDA levels. (B) Catalase activity. (C) SOD activity. (D) GPx activity. Columns with different lowercase letters are significantly different ($p < 0.05$).

Furthermore, the contents of acetic acid and propionic acid were significantly reduced within HFD-treated mice, whereas they were elevated in the H-PEP group (Fig. 12A and B). Interestingly, the lower butyric acid level in HFD-fed mice was significantly restored by administering atorvastatin and PEP (Fig. 12C). A similar trend was observed in the contents of total SCFAs among the groups (Fig. 12D). In adipose tissue, GPR41 and GPR43 are predominantly expressed in adipocytes and have been shown to play a role in accelerating lipid metabolism and energy expenditure.[19] As anticipated, lower expression of GPR41 and GPR43 was observed in the epididymal adipose tissues of the HFD group, which was recovered by atorvastatin and PEP treatment (Fig. 12E and F).

3.7. The dominant microbiota was identified using Spearman correlation coefficient analysis

Spearman's correlation analysis was presented using heatmaps and network construction, revealing the correlation between the gut microbiota and biochemical parameters. As shown in Fig. 13A, 13 floras at the genus level were highly correlated with obesity biomarkers in this study. Seven harmful bacteria were identified: *[Eubacterium]_coprostanoligenes_group* (positively correlated with food intake, ALT, HMGCR, and ACC1; negatively correlated with IL-10, fecal cholesterol, TBA, fat excretion, LXRα, and LXRβ), *Anaeroplasma* (positively correlated with food intake, HMGCR; negatively correlated with fecal TG, cholesterol, TBA, and fat excretion), *Christensenellaceae_R-7_group* (positively correlated with SREBP-1), *Clostridia_vadinBB60_group* (positively correlated with food intake; negatively with fecal fat excretion, LXRα, and LXRβ), *Erysipelatoclostridium* (positively correlated with weight gain, energy intake, EF weight, and body fat ratio; negatively correlated with propionic acid), *Lachnospiraceae_NK4A136_group* (negatively correlated with fecal TG, cholesterol, and TBA excretion), and *Ruminococcus* (positively correlated with C/EBPα; negatively correlated with IL-10 and fecal cholesterol excretion).

Conversely, six beneficial floras were observed: *Clostridium_sensu_stricto_1* (positively correlated with IL-10, fecal cholesterol excretion, and LXRα), *Desulfovibrio* (positively correlated with fecal TG excretion), *Lactobacillus* (positively correlated with IκBα and HSL; negatively correlated with weight gain, energy intake, TC, and LDL-C), *Muribaculaceae* (positively correlated with fecal TBA excretion; negatively correlated with food intake), *Romboutsia* (positively correlated with IL-10 and GPR41), and *Turicibacter* (positively correlated with fecal fat excretion; negatively correlated with food intake).

Furthermore, network construction illustrated the interactions between the gut microbiota and dominant mediators

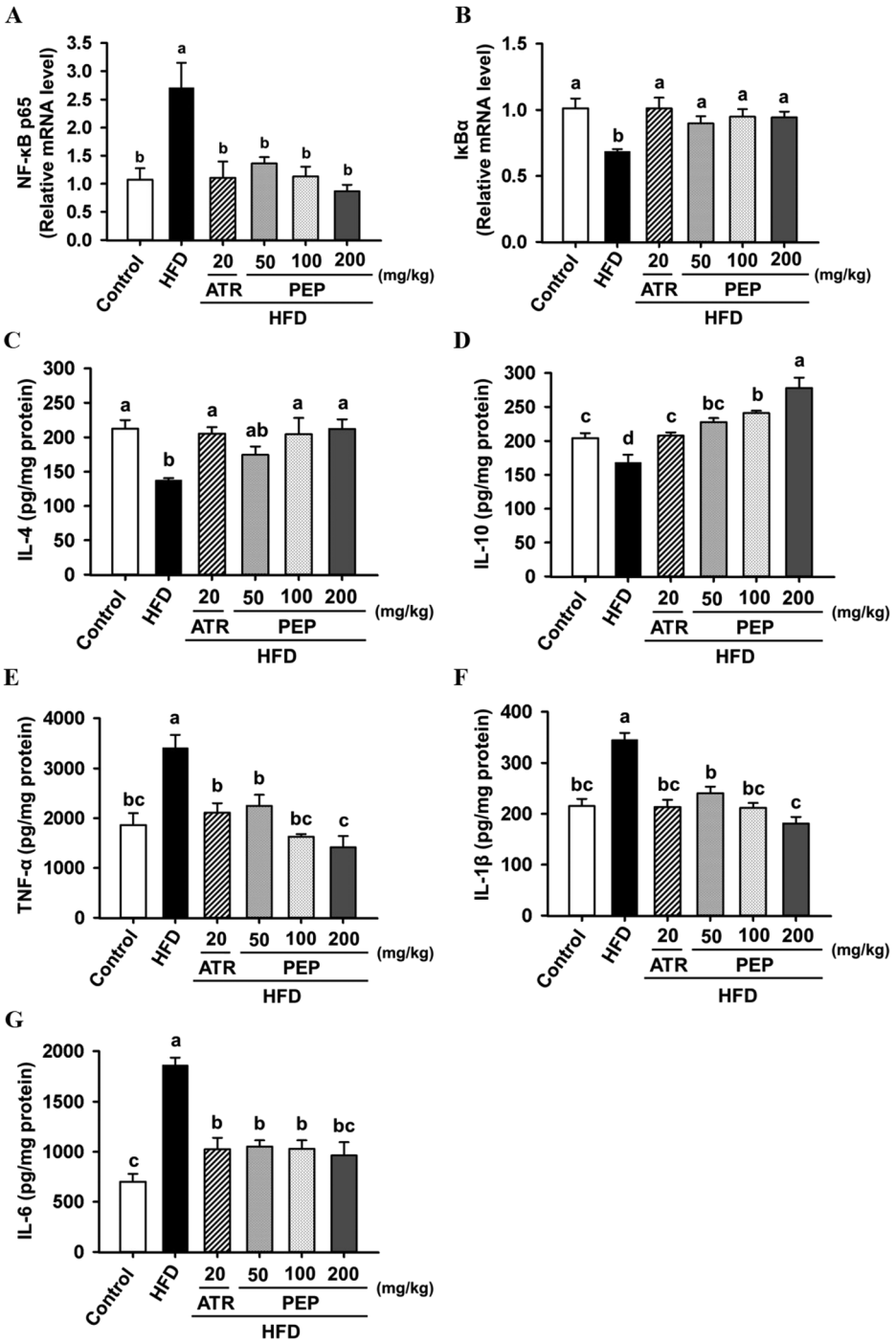

Fig. 8 Effect of PEP administration on hepatic inflammatory reaction in HFD-induced obese mice. (A and B) Hepatic mRNA expression of NF-κB and IκBα. (C–G) Cytokine expression of IL-4, IL-10, TNF-α, IL-1β, and IL-6 proteins. Columns with different lowercase letters are significantly different ($p < 0.05$).

in this study. As shown in Fig. 13B, the results revealed that crucial gut bacteria, specifically Lactobacillus, played a dominant role in lipolysis-related and anti-inflammatory pathways by reducing the lipid profile, weight gain, and energy intake. On the other hand, *Anaeroplasma* and *Clostridia_vadinBB60_group* were highly associated with food intake and cholesterol metabolism-related signaling and may obstruct fecal TG, cholesterol, TBA, and fat excretion. Polysaccharide supplementation has been documented to regulate lipid metabolic pathways and fecal fat excretion by promoting the growth of *Lactobacillus* and increasing the production of SCFAs.[20,21] On the other hand, the relative abundance of harmful bacteria, such as *Anaeroplasma* and *Clostridia_vadinBB60_group*, is significantly elevated in HFD-

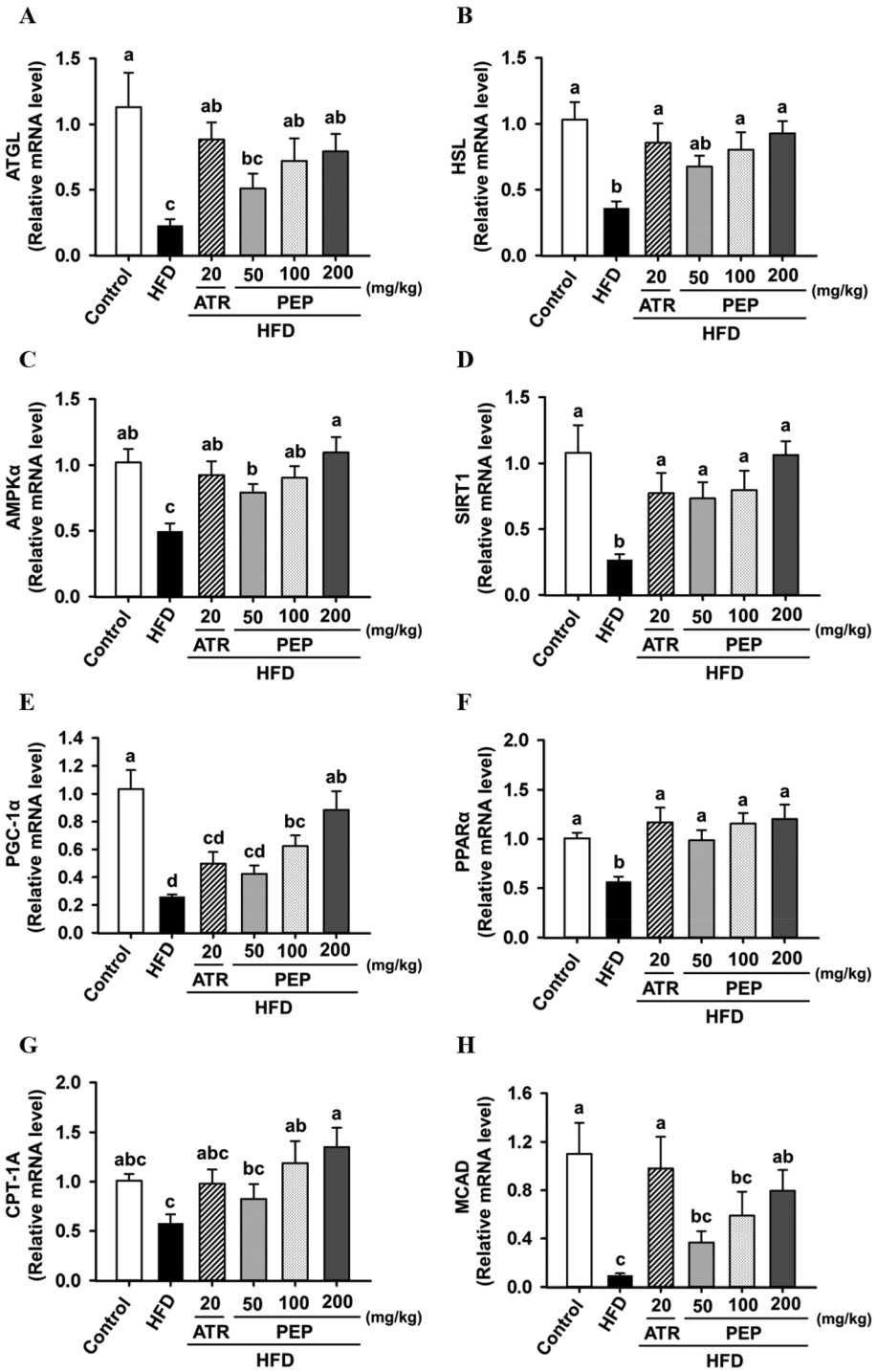

Fig. 9 Effect of PEP administration on hepatic lipolysis and β-oxidation-related gene expression in HFD-induced obese mice. Hepatic mRNA expression of (A and B) lipolysis-related genes (ATGL and HSL), (C) lipid metabolism key mediator (AMPKα), and (D-H) β-oxidation-related genes (SIRT1, PGC-1α, PPARα, CPT-1A, and MCAD). Columns with different lowercase letters are significantly different ($p < 0.05$).

fed mice and patients with non-alcoholic fatty liver disease.[22] Reliably, PEP administration promoted lipid metabolism and fecal fat excretion by enhancing the relative abundance of beneficial bacteria, such as *Lactobacillus*, while inhibiting harmful bacteria, including *Anaeroplasma* and *Clostridia_vadinBB60_group*.

4. Discussion

Dietary interventions for obesity are well-established for their safety, affordability, and effectiveness.[2] The administration of polysaccharides is highly recommended due to their capacity to modulate the gut microbiota and prevent dysbiosis in the

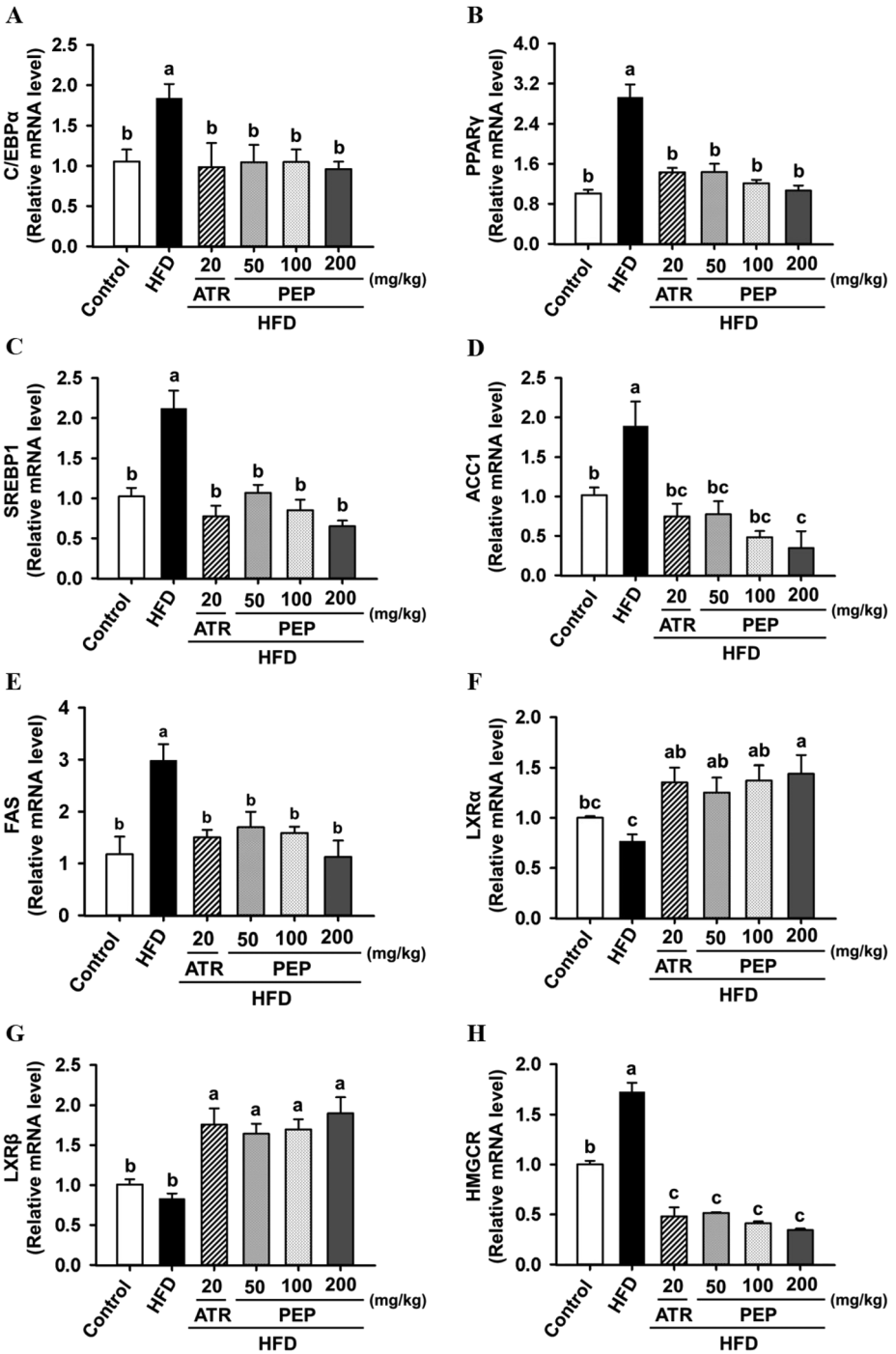

Fig. 10 Effect of PEP administration on hepatic *de novo* lipogenesis and cholesterol metabolism gene expression in HFD-induced obese mice. Hepatic mRNA expression of (A–E) *de novo* lipogenesis-related genes (C/EBPα, PPARγ, SREBP1, ACC1, and FAS) and (F–H) cholesterol metabolism-related genes (LXRα, LXRβ, and HMGCR). Columns with different lowercase letters are significantly different ($p < 0.05$).

context of HFD consumption or a Western diet.[23] Although other components from *Phyllanthus emblica* have been shown to exert anti-obesity effects,[10,11] the processes of extraction, ethanol precipitation, and purification effectively remove residual constituents such as proteins, lipids, phenolics, flavonoids, pigments, nucleic acids, and other small organic or inorganic compounds that may be conjugated with plant polysaccharides.[24] As a result of these procedures, no flavonoids or phenolic acids are detected in purified polysaccharides.[25] In this study, the observation that the middle-dose group (100 mg per kg b.w.) exhibited slightly greater anti-obesity effects than the low-dose group (50 mg per kg b.w.) may be attributed to a non-linear dose–response relationship. Biological variability among the mice may also have contributed to this unexpected

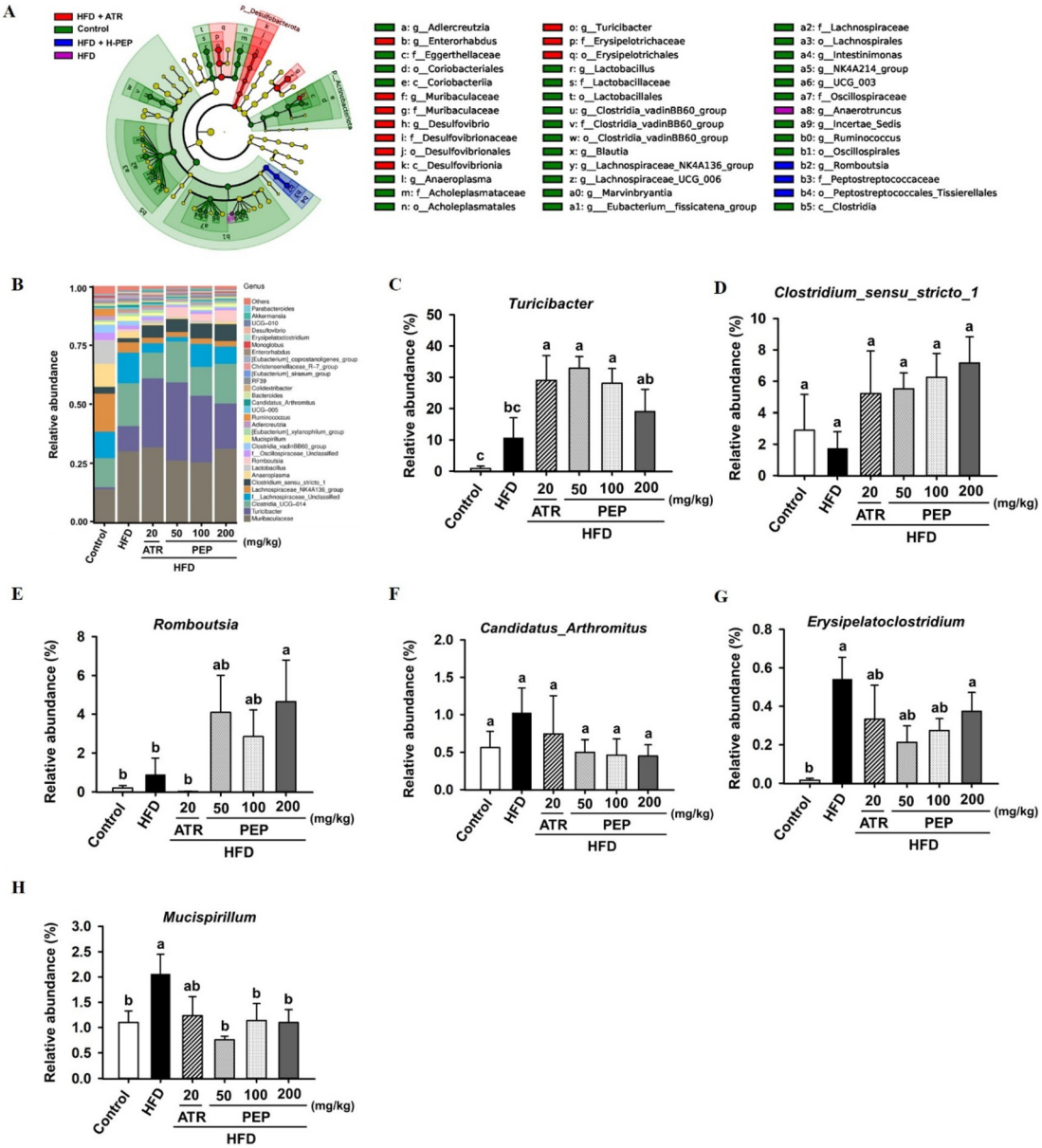

Fig. 11 Effect of PEP administration on gut microbiota modulation in HFD-induced obese mice. (A) LEfSe cladogram showing the phylogenetic relationships of bacterial taxa. (B) Proportion of gut flora at the genus level in each group. (C–H) Relative abundances of *Turicibacter, Clostridium_sensu_stricto_1, Romboutsia, Candidatus_Arthromitus, Erysipelatoclostridium,* and *Mucispirillum*. Columns with different lowercase letters are significantly different ($p < 0.05$).

trend.[26,27] Additionally, the high-dose group (200 mg per kg b. w.) demonstrated the most pronounced obesity-mitigating effects among all groups, suggesting that this dosage may have reached the threshold required for optimal activation of specific metabolic or signaling pathways. Similar non-linear dose–response patterns in obesity attenuation have been reported in other polysaccharide treatment studies.[12,28,29]

While several pharmacological treatments for obesity, such as Orlistat, Liraglutide, and the Naltrexone/Bupropion combination, have been approved by the FDA, their use is frequently accompanied by adverse effects, including headaches, gastrointestinal discomfort, palpitations, tachycardia, anxiety, and elevated blood pressure.[30–34] In contrast, eight weeks of PEP supplementation in this study did not induce hepatotoxicity or nephrotoxicity in mice, highlighting its potential as a safer alternative for obesity management. Indeed, this study demonstrated that PEP administration attenuated obesity by reshaping intestinal flora, inhibiting inflammation and oxidative stress, and accelerating lipid metabolism.

Dietary habits strongly influence the composition of the gut microbiota.[35,36] The gut microbiota is inextricably linked to maintaining homeostasis by regulating oxidative stress, immune response, lipid metabolism, and effectively modifying

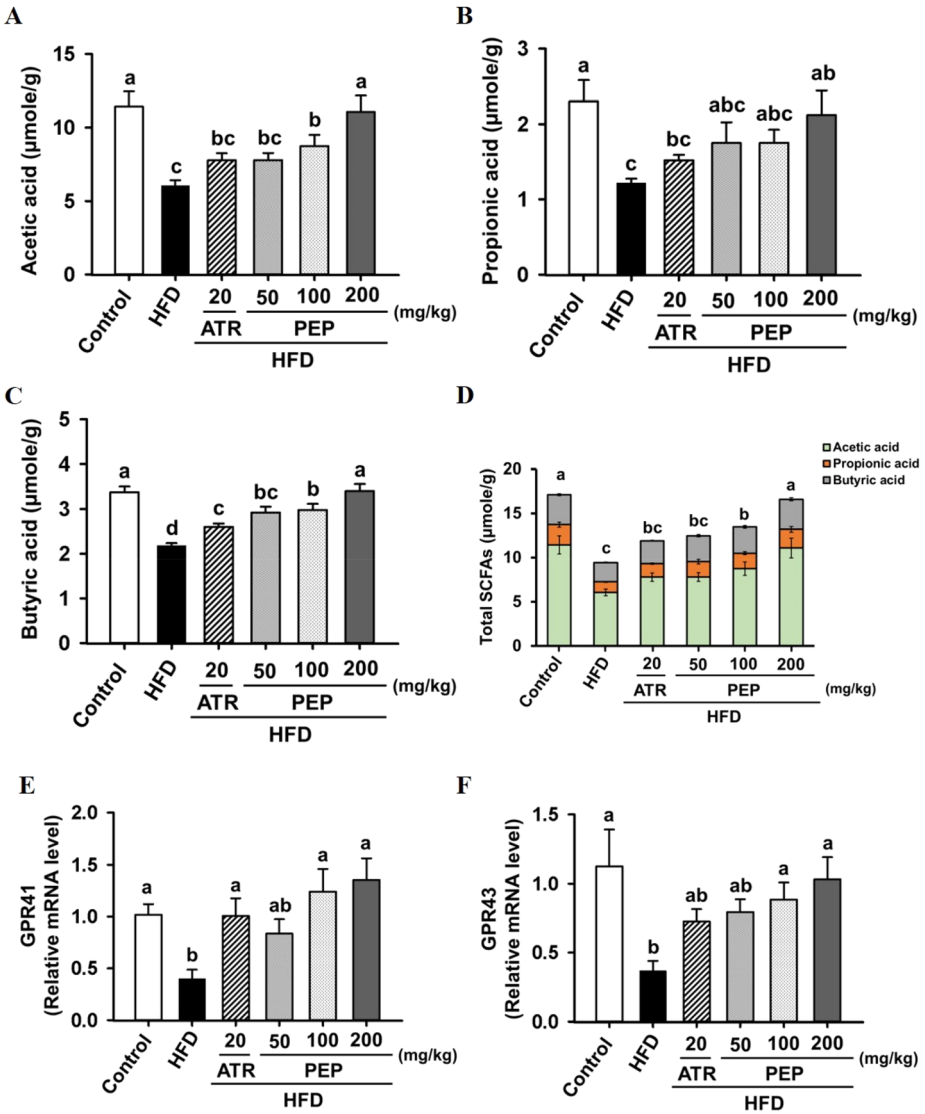

Fig. 12 Effect of PEP administration on SCFA production and mRNA levels of the receptors in HFD-induced obese mice. (A–D) Contents of acetic acid, propionic acid, butyric acid, and total SCFAs. (E and F) mRNA expression of GPR41 and GPR43 in epididymal adipose tissue. Columns with different lowercase letters are significantly different ($p < 0.05$).

blood glucose levels.[11,37] In this study, seven obesity-promoting bacteria (*[Eubacterium]_coprostanoligenes_group*, *Anaeroplasma*, *Christensenellaceae_R-7_group*, *Clostridia_vadinBB60_group*, *Erysipelatoclostridium*, *Lachnospiraceae_NK4A136_group*, and *Ruminococcus*) and six obesity-repressed floras (*Clostridium_sensu_stricto_1*, *Desulfovibrio*, *Lactobacillus*, *Muribaculaceae*, *Romboutsia*, and *Turicibacter*) were noted.

Previous evidence has shown that the *[Eubacterium]_coprostanoligenes_group* and *Anaeroplasma* bacteria are signature genera in the gut microbiota ecosystem, involved in the development of dyslipidemia with abnormal obesity indicators (body weight, TC, TG, LDL-C, AST, and ALT) following HFD supplementation.[38–40] Moreover, it has been reported that the levels of serum lipid profiles (TG, TC, and LDL-C) are significantly positively correlated with the *Christensenellaceae_R-7_group*. In contrast, the flora negatively correlates with SCFA production.[41] The *Clostridia_vadinBB60_group* increased significantly due to the induction of the HFD[42] and could contribute to muscular fat deposition.[43] Furthermore, the enrichment of *Erysipelatoclostridium* is strongly correlated with body weight gain, fat accumulation, TC, TG, LDL-C, blood glucose, MDA, TNF-α, IL-6, and the activation of *de novo* lipogenesis-related genes (PPARγ, SREBP1, and FAS), making it a harmful bacterium for promoting obesity.[44–46] Furthermore, polysaccharides from *Sporidiobolus pararoseus* significantly reduce the abundance of obesity-promoting *Lachnospiraceae NK4A136* bacteria.[47] Additionally, *Ruminococcus* is enriched in obese mice and associated with metabolic syndrome and weight gain.[48] In agreement with the above evidence, this study found that all the harmful floras were positively correlated with obesity indicators, including food intake, weight gain, energy intake, epididymal fat weight, body fat ratio, ALT, HMGCR, ACC1, and C/

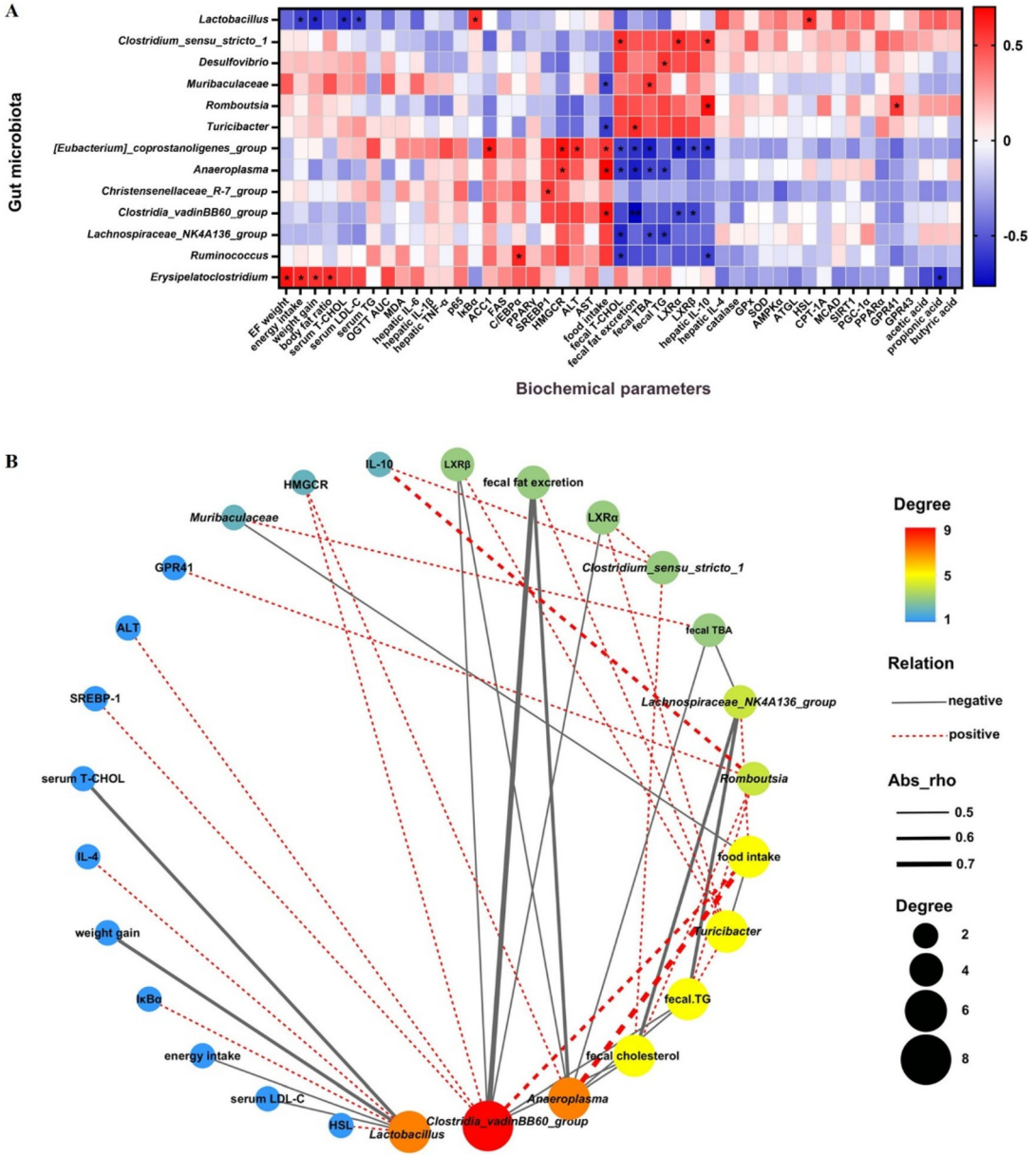

Fig. 13 Effect of PEP administration on Spearman correlation and network construction between obesity-related parameters and the gut microbiota. (A) Heatmap of Spearman's rank correlation (red = positive correlation; blue = negative correlation, $*p < 0.05$ and $**p < 0.01$). (B) Network construction. Larger circles and red color represent stronger correlations. Red lines indicate positive correlations. Gray lines indicate negative correlations.

EBPα, which were suppressed by PEP administration in HFD-fed mice.

In contrast, *Clostridium_sensu_stricto_1* and *Romboutsia* positively affect SCFA production and immune regulation, helping suppress serum TNF-α levels and delay diabetes.[49–51] Additionally, *Turicibacter* strains reduce serum TC, TG, and adipose tissue mass.[52] Furthermore, *Muribaculaceae* is an important source of SCFAs that can improve pancreatic beta-cell function, enhance glycolipid metabolic parameters (TC, insulin resistance, and AUC), alter primary bile acid biosynthesis, and reduce the release of proinflammatory cytokines.[53] Notably, the increase in beneficial bacteria was significantly positively correlated with lipid metabolism indicators (fecal fat, TC, TG, TBA excretion, LXRα, and HSL) and anti-inflammatory markers (IL-10 and IκBα), suggesting that PEP ameliorates obesity through the modulation of the gut microbiota.

HFD-caused obesity and associated lipid dysmetabolism in mice, where elevated circulating levels of free fatty acids drive inflammation, adipogenesis, and oxidative stress, contribute to obesity-related diseases.[54,55] Simultaneously, natural polysaccharides have been reported to alleviate diet-induced obesity by improving lipid and energy metabolism, suppres-

sing appetite, and directly inhibiting inflammation and oxidative stress.[4] For instance, tea polysaccharides from Tianzhu Xianyue fried green tea repressed lipogenesis and promoted lipolysis by downregulating SREBP-1 and FAS and upregulating HSL and ATGL in HFD-fed ApoE$^{-/-}$ mice.[56] Moreover, oral administration of chicory (*Cichorium intybus* L.) polysaccharides in HFD-induced NAFLD rats significantly enhanced hepatic lipolysis (ATGL and AMPKα) and β-oxidation (CPT-1) while reducing *de novo* lipogenesis markers (ACC1 and FAS) and levels of ALT, AST, TG, TC, LDL-C, glucose, and MDA.[57] Additionally, dietary polysaccharides enhance the β-oxidation of fatty acids and the activity of antioxidant enzymes (CAT, SOD, and GPx), thereby attenuating obesity by decreasing serum levels of TG, TC, LDL-C, MDA, and body weight gain.[58]

Circulating SCFAs are closely associated with reduced adipocyte lipogenesis through interaction with GPR41 and GPR43 receptors, thereby accelerating lipid metabolism and enhancing energy expenditure.[59,60] Studies have confirmed that SCFAs directly regulate immune responses, act as antioxidants, and reduce fat deposition through polysaccharides.[12,20,61] In this study, PEP treatment induced higher expression of SCFAs and GPR41/GPR43 in a dose-dependent manner. Similarly, key indicators related to lipolysis (ATGL, HSL, and AMPKα), β-oxidation (SIRT1, PGC-1α, PPARα, CPT-1A, and MCAD), *de novo* lipogenesis (SREBP1, ACC1, and FAS), cholesterol metabolism (LXRα and HMGCR), fecal excretion of triglycerides and cholesterol, antioxidant enzyme activity (catalase and GPx), and inflammatory mediators (NF-κB, IL-1β, and TNF-α) also exhibited a similar dose-dependent pattern. These findings suggest that PEP administration may protect against obesity by enhancing anti-inflammatory, antioxidant, and lipid metabolism activities through gut-derived SCFAs and GPR41/GPR43 signaling.

5. Conclusion

In summary, this study investigated the potential of PEP in combating obesity, focusing on its mechanisms related to lipid metabolism, antioxidant activity, anti-inflammatory effects, and modulation of the gut microbiota. PEP was found to inhibit lipid synthesis pathways, alleviating hyperlipidemia while promoting fecal lipid excretion. Additionally, PEP altered the gut microbiota composition, enhancing the production of SCFAs. These SCFAs may contribute to improved lipid metabolism and energy intake, increased fat excretion, and enhanced antioxidant and immune responses *via* GPR41/43, AMPK, and NF-κB signaling pathways. Overall, these findings highlight the potential of PEP as a functional food ingredient for preventing obesity, emphasizing its beneficial effects on lipid regulation and gut health. Despite the promising findings, several limitations require further exploration. These include a more detailed understanding of the specific role of the gut microbiota in obesity modulation and the underlying *in vivo* mechanisms associated with its other metabolites. Further clinical research in these areas is crucial for fully optimizing the potential of PEP and gaining a more comprehensive understanding of its effects, paving the way for its broader application.

Abbreviations

ATR	Atorvastatin
CPT-1	Carnitine palmitoyl transferase 1
HMGCR	3-Hydroxy-3-methylglutaryl coenzyme A reductase
HSL	Hormone-sensitive lipase
LXR	Liver X receptor
MCAD	Medium-chain acyl-CoA dehydrogenase
PEP	*Phyllanthus emblica* L. polysaccharides
PGC-1α	Peroxisome proliferator-activated receptor γ coactivator-1α
SIRT1	NAD-dependent deacetylase sirtuin-1
SREBP1	Sterol regulatory element-binding protein-1.

Author contributions

YH Hsu: conceptualization, data curation, investigation, and methodology. SY Chen: validation and writing – original draft. JD Chen: data curation and methodology. GC Yen: conceptualization, funding acquisition, and writing – review & editing. All authors read and approved the final manuscript.

Data availability

The data generated and analyzed during this study are included in this article. The data that support the findings of this study are available from the corresponding author upon reasonable request. The detailed primer sequences utilized for real-time PCR analysis are provided in the ESI† for further reference.

Conflicts of interest

The authors declare that they have no known competing financial interests or personal relationships that could have appeared to influence the work reported in this paper.

Acknowledgements

This research was financially supported in part by grant 112AS-1.7.1-FD-Z2(1) from the Agriculture and Food Agency, Ministry of Agriculture, Taiwan, and by the "Advanced Plant and Food Crop Biotechnology Center" from The Featured Areas Research Center Program within the framework of the Higher Education Sprout Project by the Ministry of Education (MOE), Taiwan.

References

1 A. Okunogbe, R. Nugent, G. Spencer, J. Powis, J. Ralston and J. Wilding, Economic impacts of overweight and obesity: Current and future estimates for 161 countries, *BMJ Glob. Health*, 2022, **7**, e009773.
2 M. Yannakoulia and N. Scarmeas, Diets, *N. Engl. J. Med.*, 2024, **390**, 2098–2106.
3 T. Jess, Microbiota, antibiotics, and obesity, *N. Engl. J. Med.*, 2014, **371**, 2526–2528.
4 C. Tang, Y. Wang, D. Chen, M. Zhang, J. Xu, C. Xu, J. Liu, J. Kan and C. Jin, Natural polysaccharides protect against diet-induced obesity by improving lipid metabolism and regulating the immune system, *Food Res. Int.*, 2023, **172**, 113192.
5 D. Tian, X. Zhong, L. Fu, W. Zhu, X. Liu, Z. Wu, Y. Li, X. Li, X. Li, X. Tao, Q. Wei, X. Yang and Y. Huang, Therapeutic effect and mechanism of polysaccharides from *Anoectochilus Roxburghii* (Wall.) Lindl. in diet-induced obesity, *Phytomedicine*, 2022, **99**, 154031.
6 A. Lovegrove, C. H. Edwards, I. De Noni, H. Patel, S. N. El, T. Grassby, C. Zielke, M. Ulmius, L. Nilsson, P. J. Butterworth, P. R. Ellis and P. R. Shewry, Role of polysaccharides in food, digestion, and health, *Crit. Rev. Food Sci. Nutr.*, 2017, **57**, 237–253.
7 K. Rekha, B. Venkidasamy, R. Samynathan, P. Nagella, M. Rebezov, M. Khayrullin, E. Ponomarev, A. Bouyahya, T. Sarkar, M. A. Shariati, M. Thiruvengadam and J. Simal-Gandara, Short-chain fatty acid: An updated review on signaling, metabolism, and therapeutic effects, *Crit. Rev. Food Sci. Nutr.*, 2024, **64**, 2461–2489.
8 Q. G. Ma, L. Wang, R. H. Liu, J. B. Yuan, H. Xiao, Z. Y. Shen, J. X. Li, J. Z. Guo, L. Cao, H. L. Huang and R. R. Wei, *Phyllanthus emblica* Linn: A comprehensive review of botany, traditional uses, phytonutrients, health benefits, quality markers, and applications, *Food Chem.*, 2024, **446**, 138891.
9 Y. Y. Chen, S. Y. Chen, J. A. Lin and G. C. Yen, Preventive effect of Indian gooseberry (*Phyllanthus emblica* L.) fruit extract on cognitive decline in high-fat diet (HFD)-fed rats, *Mol. Nutr. Food Res.*, 2023, **67**, e2200791.
10 S. Y. Chen, Y. N. Huang, J. A. Lin and G. C. Yen, Effect of Indian gooseberry extract on improving methylglyoxal-associated leptin resistance in peripheral tissues of high-fat diet-fed rats, *J. Food Drug Anal.*, 2024, **32**, 54–64.
11 H. Y. Chang, S. Y. Chen, J. A. Lin, Y. Y. Chen, Y. Y. Chen, Y. C. Liu and G. C. Yen, *Phyllanthus emblica* fruit improves obesity by reducing appetite and enhancing mucosal homeostasis via the gut microbiota-brain-liver axis in HFD-induced leptin-resistant rats, *J. Agric. Food Chem.*, 2024, **72**, 10406–10419.
12 D. Yuan, Q. Huang, C. Li and X. Fu, A polysaccharide from *Sargassum pallidum* reduces obesity in high-fat diet-induced obese mice by modulating glycolipid metabolism, *Food Funct.*, 2022, **13**, 7181–7191.
13 Y. C. Liu, S. Y. Chen, Y. Y. Chen, H. Y. Chang, I. C. Chiang and G. C. Yen, Polysaccharides extracted from common buckwheat (*Fagopyrum esculentum*) attenuate cognitive impairment via suppressing RAGE/p38/NF-kappaB signaling and dysbiosis in AlCl3-treated rats, *Int. J. Biol. Macromol.*, 2024, **276**, 133898.
14 Y. Xu, N. Liu, X. Fu, L. Wang, Y. Yang, Y. Ren, J. Liu and L. Wang, Structural characteristics, biological, rheological and thermal properties of the polysaccharide and the degraded polysaccharide from raspberry fruits, *Int. J. Biol. Macromol.*, 2019, **132**, 109–118.
15 J. Hu, J. Bi, W. Wang and X. Li, Comparison of characterization and composition of melanoidins from three different dried apple slices, *Food Chem.*, 2024, **455**, 139890.
16 G. R. Steinberg and D. G. Hardie, New insights into activation and function of the AMPK, *Nat. Rev. Mol. Cell Biol.*, 2023, **24**, 255–272.
17 X. Hu, F. Chen, L. Jia, A. Long, Y. Peng, X. Li, J. Huang, X. Wei, X. Fang, Z. Gao, M. Zhang, X. Liu, Y. G. Chen, Y. Wang, H. Zhang and Y. Wang, A gut-derived hormone regulates cholesterol metabolism, *Cell*, 2024, **187**, 1685–1700.
18 K. Guo, C. Figueroa-Romero, M. Noureldein, L. M. Hinder, S. A. Sakowski, A. E. Rumora, H. Petit, M. G. Savelieff, J. Hur and E. L. Feldman, Gut microbiota in a mouse model of obesity and peripheral neuropathy associated with plasma and nerve lipidomics and nerve transcriptomics, *Microbiome*, 2023, **11**, 52.
19 D. H. Lee, M. T. Kim and J. H. Han, GPR41 and GPR43: From development to metabolic regulation, *Biomed. Pharmacother.*, 2024, **175**, 116735.
20 Q. Yang, S. Chang, Y. Tian, H. Zhang, Y. Zhu, W. Li and J. Ren, Simulated digestion and gut microbiota fermentation of polysaccharides from *Lactarius hatsudake* Tanaka mushroom, *Food Chem.*, 2025, **466**, 142146.
21 H. Dai, Z. Shan, L. Shi, Y. Duan, Y. An, C. He, Y. Lyu, Y. Zhao, M. Wang, Y. Du, J. Xie, Y. Yang and B. Zhao, Mulberry leaf polysaccharides ameliorate glucose and lipid metabolism disorders via the gut microbiota-bile acids metabolic pathway, *Int. J. Biol. Macromol.*, 2024, **282**, 136876.
22 S. Tian, Y. Lei, F. Zhao, J. Che, Y. Wu, P. Lei, Y. E. Kang and Y. Shan, Improving insulin resistance by sulforaphane via activating the *Bacteroides* and *Lactobacillus* SCFAs-GPR-GLP1 signal axis, *Food Funct.*, 2024, **15**, 8644–8660.
23 W. Zhang, L. Yu, Q. Yang, J. Zhang, W. Wang, X. Hu, J. Li and G. Zheng, Smilax China L. polysaccharide prevents HFD induced-NAFLD by regulating hepatic fat metabolism and gut microbiota, *Phytomedicine*, 2024, **127**, 155478.
24 M. M. Ahmad, S. A. S. Chatha, Y. Iqbal, A. I. Hussain, I. Khan and F. W. Xie, Recent trends in extraction, purification, and antioxidant activity evaluation of plant leaf-extract polysaccharides, *Biofuels, Bioprod. Biorefin.*, 2022, **16**, 1820–1848.
25 S. C. Chang, B. Y. Hsu and B. H. Chen, Structural characterization of polysaccharides from *Zizyphus jujuba* and evaluation of antioxidant activity, *Int. J. Biol. Macromol.*, 2010, **47**, 445–453.

26 P. T. Vedell, K. L. Svenson and G. A. Churchill, Stochastic variation of transcript abundance in C57BL/6J mice, *BMC Genomics*, 2011, **12**, 167.
27 J. Freund, A. M. Brandmaier, L. Lewejohann, I. Kirste, M. Kritzler, A. Kruger, N. Sachser, U. Lindenberger and G. Kempermann, Emergence of individuality in genetically identical mice, *Science*, 2013, **340**, 756–759.
28 Y. Y. Wu, Y. F. Zhang, S. S. Huang, W. F. Xie, G. N. Huang, Y. Zou, Z. W. Ye, T. Wei, J. F. Lin and Q. W. Zheng, Anti-obesity effects of the high molecular weight *Cordyceps militaris* polysaccharide CMP40 in high-fat diet mice, *Food Biosci.*, 2024, **60**, 104467.
29 L. Li, L. Ma, Y. Wen, J. Xie, L. Yan, A. Ji, Y. Zeng, Y. Tian and J. Sheng, Crude polysaccharide extracted from *Moringa oleifera* leaves prevents obesity in association with modulating gut microbiota in high-fat diet-fed mice, *Front. Nutr.*, 2022, **9**, 861588.
30 E. S. Siraj and K. J. Williams, Liraglutide in weight management, *N. Engl. J. Med.*, 2015, **373**, 1782.
31 X. Pi-Sunyer, C. M. Apovian, S. L. McElroy, E. Dunayevich, L. M. Acevedo and F. L. Greenway, Psychiatric adverse events and effects on mood with prolonged-release naltrexone/bupropion combination therapy: A pooled analysis, *Int. J. Obes.*, 2019, **43**, 2085–2094.
32 S. E. Nissen, K. E. Wolski, L. Prcela, T. Wadden, J. B. Buse, G. Bakris, A. Perez and S. R. Smith, Effect of naltrexone-bupropion on major adverse cardiovascular events in overweight and obese patients with cardiovascular risk factors: A randomized clinical trial, *J. Am. Med. Assoc.*, 2016, **315**, 990–1004.
33 I. J. Douglas, J. Langham, K. Bhaskaran, R. Brauer and L. Smeeth, Orlistat and the risk of acute liver injury: Self controlled case series study in UK Clinical Practice Research Datalink, *Br. Med. J.*, 2013, **346**, f1936.
34 B. Buysschaert, S. Aydin, J. Morelle, M. P. Hermans, M. Jadoul and N. Demoulin, Weight loss at a high cost: Orlistat-induced late-onset severe kidney disease, *Diabetes Metab.*, 2016, **42**, 62–64.
35 T. Yatsunenko, F. E. Rey, M. J. Manary, I. Trehan, M. G. Dominguez-Bello, M. Contreras, M. Magris, G. Hidalgo, R. N. Baldassano, A. P. Anokhin, A. C. Heath, B. Warner, J. Reeder, J. Kuczynski, J. G. Caporaso, C. A. Lozupone, C. Lauber, J. C. Clemente, D. Knights, R. Knight and J. I. Gordon, Human gut microbiome viewed across age and geography, *Nature*, 2012, **486**, 222–227.
36 L. A. David, C. F. Maurice, R. N. Carmody, D. B. Gootenberg, J. E. Button, B. E. Wolfe, A. V. Ling, A. S. Devlin, Y. Varma, M. A. Fischbach, S. B. Biddinger, R. J. Dutton and P. J. Turnbaugh, Diet rapidly and reproducibly alters the human gut microbiome, *Nature*, 2014, **505**, 559–563.
37 D. Zeevi, T. Korem, N. Zmora, D. Israeli, D. Rothschild, A. Weinberger, O. Ben-Yacov, D. Lador, T. Avnit-Sagi, M. Lotan-Pompan, J. Suez, J. A. Mahdi, E. Matot, G. Malka, N. Kosower, M. Rein, G. Zilberman-Schapira, L. Dohnalova, M. Pevsner-Fischer, R. Bikovsky, Z. Halpern, E. Elinav and E. Segal, Personalized nutrition by prediction of glycemic responses, *Cell*, 2015, **163**, 1079–1094.
38 H. Zeng, S. L. Ishaq, Z. Liu and M. R. Bukowski, Colonic aberrant crypt formation accompanies an increase of opportunistic pathogenic bacteria in C57BL/6 mice fed a high-fat diet, *J. Nutr. Biochem.*, 2018, **54**, 18–27.
39 W. Wei, W. Jiang, Z. Tian, H. Wu, H. Ning, G. Yan, Z. Zhang, Z. Li, F. Dong, Y. Sun, Y. Li, T. Han, M. Wang and C. Sun, Fecal *g. Streptococcus* and *g. Eubacterium_coprostanoligenes_group* combined with sphingosine to modulate the serum dyslipidemia in high-fat diet mice, *Clin. Nutr.*, 2021, **40**, 4234–4245.
40 K. Dai, Y. Song, D. Zhang, Y. Wei, S. Jiang, F. Xu, H. Wang, X. Zhang and X. Shao, Thinned peach polyphenols alleviate obesity in high fat mice by affecting gut microbiota, *Food Res. Int.*, 2022, **157**, 111255.
41 Y. Wang, W. Yao, B. Li, S. Qian, B. Wei, S. Gong, J. Wang, M. Liu and M. Wei, Nuciferine modulates the gut microbiota and prevents obesity in high-fat diet-fed rats, *Exp. Mol. Med.*, 2020, **52**, 1959–1975.
42 B. H. Lee, K. T. Hsu, Y. Z. Chen, Y. L. Tain, C. Y. Hou, Y. C. Lin and W. H. Hsu, Polysaccharide extracts derived from defloration waste of fruit pitaya regulates gut microbiota in a mice model, *Fermentation*, 2022, **8**, 108.
43 P. Guo, S. Lin, Q. Lin, S. Wei, D. Ye and J. Liu, The digestive tract histology and geographical distribution of gastrointestinal microbiota in yellow-feather broilers, *Poult. Sci.*, 2023, **102**, 102844.
44 J. Ye, Y. Zhao, X. Chen, H. Zhou, Y. Yang, X. Zhang, Y. Huang, N. Zhang, E. M. K. Lui and M. Xiao, Pu-erh tea ameliorates obesity and modulates gut microbiota in high fat diet fed mice, *Food Res. Int.*, 2021, **144**, 110360.
45 L. Sun, L. Ma, Y. Ma, F. Zhang, C. Zhao and Y. Nie, Insights into the role of gut microbiota in obesity: pathogenesis, mechanisms, and therapeutic perspectives, *Protein Cell*, 2018, **9**, 397–403.
46 Y. Ma, L. Zhu, H. Ke, S. Jiang and M. Zeng, Oyster (*Crassostrea gigas*) polysaccharide ameliorates obesity in association with modulation of lipid metabolism and gut microbiota in high-fat diet fed mice, *Int. J. Biol. Macromol.*, 2022, **216**, 916–926.
47 B. Hu, C. Liu, W. Jiang, H. Zhu, H. Zhang, H. Qian and W. Zhang, Chronic *in vitro* fermentation and *in vivo* metabolism: Extracellular polysaccharides from *Sporidiobolus pararoseus* regulate the intestinal microbiome of humans and mice, *Int. J. Biol. Macromol.*, 2021, **192**, 398–406.
48 X. Feng, M. Guo, J. Li, Z. Shen, F. Mo, Y. Tian, B. Wang and C. Wang, The structural characterization of a novel Chinese yam polysaccharide and its hypolipidemic activity in HFD-induced obese C57BL/6J mice, *Int. J. Biol. Macromol.*, 2024, **265**, 130521.
49 Y. Zhao, S. Yu, H. Zhao, L. Li, Y. Li, M. Liu and L. Jiang, Integrated multi-omics analysis reveals the positive leverage of citrus flavonoids on hindgut microbiota and host homeostasis by modulating sphingolipid metabolism in

mid-lactation dairy cows consuming a high-starch diet, *Microbiome*, 2023, **11**, 236.

50 X. Wu, J. Cao, M. Li, P. Yao, H. Li, W. Xu, C. Yuan, J. Liu, S. Wang, P. Li and Y. Wang, An integrated microbiome and metabolomic analysis identifies immunoenhancing features of *Ganoderma lucidum* spores oil in mice, *Pharmacol. Res.*, 2020, **158**, 104937.

51 Y. Chen, Y. Ouyang, X. Chen, R. Chen, Q. Ruan, M. A. Farag, X. Chen and C. Zhao, Hypoglycaemic and anti-ageing activities of green alga *Ulva lactuca* polysaccharide via gut microbiota in ageing-associated diabetic mice, *Int. J. Biol. Macromol.*, 2022, **212**, 97–110.

52 J. B. Lynch, E. L. Gonzalez, K. Choy, K. F. Faull, T. Jewell, A. Arellano, J. Liang, K. B. Yu, J. Paramo and E. Y. Hsiao, Gut microbiota *Turicibacter* strains differentially modify bile acids and host lipids, *Nat. Commun.*, 2023, **14**, 3669.

53 J. Deng, X. Zou, Y. Liang, J. Zhong, K. Zhou, J. Zhang, M. Zhang, Z. Wang, Y. Sun and M. Li, Hypoglycemic effects of different molecular weight konjac glucomannans via intestinal microbiota and SCFAs mediated mechanism, *Int. J. Biol. Macromol.*, 2023, **234**, 122941.

54 S. R. Shaikh, M. A. Beck, Y. Alwarawrah and N. J. MacIver, Emerging mechanisms of obesity-associated immune dysfunction, *Nat. Rev. Endocrinol.*, 2024, **20**, 136–148.

55 V. Las Heras, S. Melgar, J. MacSharry and C. G. M. Gahan, The influence of the Western diet on microbiota and gastrointestinal immunity, *Annu. Rev. Food Sci. Technol.*, 2022, **13**, 489–512.

56 D. D. Kuang, X. Y. Li, X. P. Qian, T. Zhang, Y. Y. Deng, Q. M. Li, J. P. Luo and X. Q. Zha, Tea polysaccharide ameliorates high-fat diet-induced renal tubular ectopic lipid deposition via regulating the dynamic balance of lipogenesis and lipolysis, *J. Agric. Food Chem.*, 2024, **72**, 12582–12595.

57 Y. Wu, F. Zhou, H. Jiang, Z. Wang, C. Hua and Y. Zhang, Chicory (*Cichorium intybus* L.) polysaccharides attenuate high-fat diet induced non-alcoholic fatty liver disease via AMPK activation, *Int. J. Biol. Macromol.*, 2018, **118**, 886–895.

58 D. Yin, Y. Zhong, H. Liu and J. Hu, Lipid metabolism regulation by dietary polysaccharides with different structural properties, *Int. J. Biol. Macromol.*, 2024, **270**, 132253.

59 Y. Yao, X. Cai, W. Fei, Y. Ye, M. Zhao and C. Zheng, The role of short-chain fatty acids in immunity, inflammation and metabolism, *Crit. Rev. Food Sci. Nutr.*, 2022, **62**, 1–12.

60 M. Nshanian, J. J. Gruber, B. S. Geller, F. Chleilat, S. M. Lancaster, S. M. White, L. Alexandrova, J. M. Camarillo, N. L. Kelleher, Y. Zhao and M. P. Snyder, Short-chain fatty acid metabolites propionate and butyrate are unique epigenetic regulatory elements linking diet, metabolism and gene expression, *Nat. Metab.*, 2025, **7**, 196–211.

61 Y. Y. Ding, J. Lan, Y. Wang, Y. Pan, T. Song, S. Liu, Z. Gu and Y. Ge, Structure characterization of *Grifola frondosa* polysaccharide and its effect on insulin resistance in HFD-fed mice, *NPJ Sci. Food*, 2025, **9**, 3.